Received 11 December 2023; accepted 10 January 2024. Date of publication 15 January 2024; date of current version 1 February 2024.

Digital Object Identifier 10.1109/OJCOMS.2024.3354074

Leveraging Edge Computing for Minimizing Base Station Energy Consumption in Multi-Cell (N)OMA Downlink Systems

MATEEN ASHRAF [1], TANELI RIIHONEN [1] (Senior Member, IEEE), AND KYUNG GEUN LEE [2]

[1] Faculty of Information Technology and Communication Sciences, Tampere University, 33014 Tampere, Finland

[2] Faculty of Information and Communication Engineering, Sejong University, Gwangjin 05006, South Korea

CORRESPONDING AUTHOR: M. ASHRAF (e-mail: mateen.ashraf@tuni.fi)

This work was supported in part by the Research Council of Finland under Grant 341489 and Grant 346622, and in part by the MSCA Individual Fellowship Grant HE/MSCA/PF/RISESWCS under Grant 3122107182.

ABSTRACT In this paper, we suggest that the combination of edge computing in the form of data compression with communication at the base stations (BSs) for transmissions to their associated multiple downlink users (DUs) is advantageous for minimizing the total energy consumption. We assume that the individual DUs have minimum rate requirements along with outage probability constraints. Then, we set the resource allocation to minimize the total energy consumption (the sum of compression energy and transmission energy) for the BSs with orthogonal and non-orthogonal multiple access (OMA and NOMA) transmission schemes, while taking into account the quality of service (QoS) constraints of individual DUs. The formulated optimization problems are non-convex and difficult to solve. Therefore, the energy minimization problems are decomposed into smaller problems and low-complexity solutions are obtained. Specifically, for the *single-cell scenario* we use Lagrange duality theory and Karush–Kuhn–Tucker conditions to obtain closed-form global optimal solutions. It is revealed that the optimal resource allocation at the BS is determined by a DU-specific parameter, named *path-loss factor*. This finding is then used to obtain the optimal resource allocation for the *multi-cell scenario* and two iterative algorithms, with guaranteed convergence, are proposed to solve the energy minimization problems for NOMA and OMA transmission schemes. Next, the effectiveness of the proposed approaches are demonstrated with the help of simulation results. It is found that the BSs can exploit the flexibilities in minimum rate requirements and outage probability requirements, and compress the data of individual DUs before transmission in an attempt toward reducing the total consumed energy.

INDEX TERMS Data compression, edge computing, energy minimization, non-orthogonal multiple access, orthogonal multiple access, power allocation.

I. INTRODUCTION

THE CONTEMPORARY wireless communication systems such as 4G, 5G and the upcoming 6G wireless communication systems have very high requirements for spectral efficiency and energy efficiency. To fulfill these demands, many new technologies have been proposed recently. Some examples of these new wireless technologies include ultra dense networks [1], milimeter wave communication [2], multiple input multiple output (MIMO) [3], heterogeneous networks (HetNets) [4], reconfigurable intelligent surfaces (RIS) [5], and visible light communication (VLC) [6], just to name a few.

Among emerging concepts, the non-orthogonal multiple access (NOMA) technique for multiuser communication has received great attention from the wireless communication research community. As the name suggests, NOMA accommodates multiple users in same frequency/time resource blocks [1]. Hence, the use of NOMA helps in substantially

improving the spectral efficiency of the communication system. In fact, it has been proven that if there is a greater variation in the channel gains of users, then NOMA can outperform orthogonal multiple access (OMA) in terms of total achievable data rate [7]. Due to its superior performance over OMA, NOMA has also been used as the access scheme in mobile edge computing [8], and Internet of Things (IoT) systems [9] in addition to the wireless communication systems.

A. RELATED WORK

The existing literature on resource allocation, which is one of main themes in this article, for NOMA can be categorized into two following categories: i) data rate maximizing power allocation, ii) power (energy efficiency) minimizing (maximizing) power allocation [1], [2], [3], [4], [5], [6], [7]. The recent research endeavors [8], [9], [10], [11], [12], [13], [14] considered different system models while incorporating NOMA transmissions for serving multiple users with the aim to maximize the total data rate. A user selection and power allocation scheme was proposed in [10] for the downlink NOMA system. Their proposed scheme maximizes the sum rate while guaranteeing latency constraints of users. On the other hand, a rate maximizing scheme was proposed in [11] while considering the individual minimum rate requirements of the users. A weighted sum rate maximizing power allocation scheme for two users was developed in [12] and closed-form expressions were obtained for individual user power allocations. While the above schemes aimed at instantaneous sum rate maximization, in [13], [14], online schemes for sum rate maximization over the long-term were proposed with the help of Lyapunov optimization techniques.

For multicarrier systems, a rate maximizing subcarrier and power allocation scheme was proposed in [15]. The data rate performance of NOMA system largely depends on the variations in the channel gains among different users. Therefore, an efficient user pairing scheme was devised in [16] and then a power control algorithm was proposed to maximize the data rate performance of the system. In order to better exploit the channel variations, the authors of [17] proposed two resource-user assignment methods to maximize the network-wide data rate based objective function. Then, an alternative direction method of multipliers based algorithm was proposed for efficient power allocation among users.

In the realm of more modern physical layer technologies such as millimeter-wave, RIS, VLC and cooperative communication, research efforts have been carried out to maximize the rate performance of NOMA system. Specifically, for millimeter-wave NOMA based communication, a user grouping scheme was proposed in [18] to maximize the achievable sum rate while satisfying the minimum data rate constraints of the individual users. An RIS assisted NOMA downlink system was considered in [19], and power allocation algorithm was developed to maximize the sum data rate. In [20], the authors combined NOMA with VLC and proposed a genetic algorithm based power allocation scheme to optimize the sum data rate performance of the system. For cooperative communication systems, an amplify-and-forward relay aided NOMA scheme was investigated in [21]. Then, a joint power allocation and relay beamforming optimization algorithm was proposed to maximize the weighted sum rate of the system. While the works in [18], [19], [20], [21] focused on single-cell system models, sum rate maximization algorithm based on alternating optimization were proposed in [22] and [23] for the multi-cell scenario with and without RIS, respectively. The work in [23] is extended in [24] to account for more than two users for each cell and an individual quality of service requirement for each BS.

As the power is an expensive resource in a communication system, it is important to use it sparingly. In this regard, a total transmit power minimization algorithm was proposed in [25] for OFDM based multicarrier systems. Since user clustering is critical in power minimization, a transmit power minimization scheme was presented in [26], where the objective of power minimization was achieved by efficient power allocation and greedy user clustering scheme. A power efficient scheme was developed in [27], where RIS was used to introduce artificial disparity among the channel conditions of the users for realizing better rate gains of NOMA as compared to OMA. These schemes rely on the availability of exact channel state information (CSI) availability for their implementation. Since the exact CSI is usually unavailable, power and energy efficient schemes for NOMA system were proposed in [28] and [29], respectively, with the consideration of imperfect CSI.

In contrast to power minimization problems, where the objective function is the total consumed power, the energy efficiency maximization problems also take into account the data rate [30]. In fact, energy efficiency in wireless communication systems in defined as the ratio between the data rate and the total consumed power. In this context, [31] extended the work of [28] and devised an energy efficient power allocation scheme for NOMA system with imperfect CSI. For light fidelity (LiFi) communication systems, the authors of [32] proposed an energy efficient NOMA technique for bidirectional LiFi-IoT communication system and proved the optimal decoding orders, and derived closed-form expressions for optimal power allocation. For a multi-cell scenario, the work in [33] solved an energy efficiency maximization problem.

The above works focus on optimizing the system performance on the basis of instantaneous CSI. However, it is not only difficult to obtain the instantaneous CSI in a practical system but it is also very much likely that the acquired CSI is error prone and/or outdated [34]. Thus, resulting in overall poor performance of the system. Therefore, it is better to consider the statistical information of the channel conditions and devise the optimization algorithms accordingly.

In order to study the affects of the variations in the channel state, much research effort has been devoted

to *analyze* the performance of NOMA while using the statistical information on the CSI. An outage probability (OP) comparison between NOMA-2000 and power-domain NOMA was presented in [35]. A full duplex cooperative NOMA (CNOMA) scheme was proposed in [36] and the closed-form expression for the OP was derived. The authors of [37] studied coordinated multipoint NOMA, and derived the analytical expressions for OP with joint transmission NOMA and Alamouti NOMA. Since the mobile nodes can be randomly located, it is important to account for their locations while assessing the communication system performance. Hence, the work [38] investigated several interesting performance metrics, such as conditional success probability, coverage probability, and mean local delay in a large scale network. In a similar context, the block error rate (BLER) for short packet downlink communication was analyzed in [39] and closed form expression was derived for average BLER.

Also, there are several existing research works that consider *optimizing* the NOMA performance on the basis of statistical information of CSI. For HetNets, the average energy efficiency maximization resource allocation scheme was proposed in [40]. In particular, an iterative algorithm based on generalized Dinklebach algorithm was proposed to obtain the optimal power allocation. An optimization problem with the objective of maximizing the minimum (Max-min) success probability of downlink users (DUs) was formulated in [41] and was solved optimally through a low complexity algorithm. This work was then extended in [42] by using weighted success probability for Max-min optimization instead of using the conventional success probability. A novel threshold based selective CNOMA scheme was introduced in [43], and optimal power allocation and threshold based selection were obtained to maximize the capacity of the network.

For cognitive NOMA systems, a throughput maximization scheme subject to satisfying fairness among secondary users was developed in [9]. Since the channel estimation errors can affect the performance of massive MIMO systems, the work [44] was dedicated to maximization of energy efficiency while accounting for channel estimation error. To achieve this goal they proposed two novel transformations based on existing fractional programming framework. Due to the channel variations among users, fairness in achieved performance is also a critical issue in NOMA systems. In order to improve fairness among DUs, an alpha-fair rate-based utility maximization problem was formulated in [45] and solved through successive convex approximation with the assumption of imperfect CSI.

While the works [9], [35], [36], [37], [38], [39], [40], [41], [42], [43], [44], [45] considered challenging research problems, none of these works focused on minimizing the energy consumption of the base station (BS). The energy consumption is a critical issue in modern wireless networks where majority of the energy consumption takes place at the BS [46]. Therefore, it is of utmost importance to devise novel schemes for minimizing BS energy consumption while satisfying varying demands of the DUs.

B. MOTIVATION AND CONTRIBUTION

With the ever increasing processing capabilities of the mobile devices, it is possible that the data aimed for a particular downlink mobile device be compressed at the BS and decompressed at the mobile device after successful reception. Meanwhile, decompression at the mobile devices may only be successful if the received data rate is higher than a certain threshold.[1] Hence, the compression for a particular mobile device data at the BS must be done according to the rate requirements of the respective mobile device. Moreover, in addition to the minimum instantaneous data rate requirement, the mobile devices may also demand a certain minimum success probability for a given data rate.

Such scenario is more relevant to IoT networks where some sensors may send their uncompressed data to fusion center/BS and then the BS needs to forward that information to DUs after (possibly) performing compression for reducing its over all energy consumption. Another example scenario is where a sensor node wants to store its sensed data in compressed form at various remote cooperating cloud memory providers and then the idea is to store appropriate amount of data at these remote memory providers such that the overall energy consumption of the sensor node is minimized. Yet another futuristic scenario could be in the intelligent transportation systems, where airborne drones may collect the real-time traffic visuals and then pass it to BSs which subsequently forwards it to driver-less vehicles after compressing it. In this particular network, it may not be possible to compress the video data directly at the surveillance drones due to their battery and weight limitations. The energy consumption at the BS(s) can be reduced in these situations since transmission energy is an increasing function of the transmission data rate or duration.

In this paper, we propose (low-complexity) total energy minimization algorithms in single cell and multi-cell scenarios while considering the possibility of compression at the transmitters. For accommodating multiple DUs, we assume power-domain NOMA transmission at the BS with perfect and imperfect successive interference cancellation (SIC) at the DUs. The rational for choosing NOMA is the superior spectral efficiency of NOMA over OMA. However, due to SIC at the DUs, the decoding complexity is generally higher for NOMA as compared to OMA. To tackle this limitation, we also consider the possibility of OMA transmission at the BS. Besides, the consideration of OMA serves the purpose of a benchmark scheme.

In summary, the main contributions of the paper are listed as follows:

1. In this article, we assume that if the data rate transmitted to a downlink user is higher than its minimum data rate requirement then the compression is lossless. Hence, we assume all the desired information can be obtained at a downlink mobile device from the received compressed data after performing decompression at the mobile device as long as the transmission rate is higher than the minimum required data rate [47].

- Optimization problems are formulated for minimizing the total energy consumption through the use of compression at the BS(s) for NOMA and OMA transmissions in single and multi-cell scenarios while satisfying the QoS constraints of the DUs.
- In the single cell scenario with a given compression energy consumption, the optimal transmit powers for individual DUs are obtained in closed-form for NOMA and OMA transmissions with fixed allocation of transmission data rates. Specifically, for NOMA transmission with perfect SIC cancellation, the transmission power minimization problem is converted into a linear program and the closed-form expression for transmit powers are obtained. Furthermore, for OMA transmission, we use contradiction to obtain closed-form expression for transmit powers.
- Then, the optimal compression rate for individual DUs is obtained that minimizes the total consumed energy at the BS. This also specifies the optimal transmission data rate that must be transmitted to individual DUs for NOMA and OMA transmissions. Specifically, for a fixed compression energy consumption, the optimization problems become convex, and hence Karush-Kuhn-Tucker (KKT) conditions are used to obtain the closed-form expressions for their global optimal solutions.
- For NOMA transmission with imperfect SIC, we use the insights obtained through the analysis of perfect SIC scenario and provide closed-form near optimal solution for DUs transmit powers.
- Finally, we extend the system model to cover the multi-cell scenario. In particular, by using the important observations obtained through the analysis of the single-cell scenario we provide low complexity iterative algorithms to solve the overall energy minimization problem in multi-cell scenario with NOMA and OMA transmissions. The convergence of these algorithms is also proved theoretically.
- Simulation results are presented to demonstrate the performance improvements brought by applying the compression in single and multi-cell scenarios.

The rest of the paper is organized as follows. The system model is presented in Section II. The problem formulations is detailed in Section III. Section IV provides the solutions of the optimization problems, and the proposed algorithms for the single-cell scenario. The the proposed algorithms for multi-cell scenario are presented in Section V. Simulation results are illustrated in Section VI. Finally, the conclusions are provided in Section VII.

II. SYSTEM MODEL

We consider a downlink system with M BSs with each BS associated with $K(m)$ single antenna DUs $\forall\ m \in \{1, \ldots, M\}$. A depiction of the considered system model is shown in Fig. 1. We assume that each of the BSs can compress the transmission bits and the DUs can successfully decompress the received data if the downlink data rate is higher than a certain threshold. We consider two types of transmission schemes: NOMA and OMA. Specifically, we consider power-domain NOMA, where different DUs are multiplexed on the same frequency and time resource, and multiplexing is achieved by assigning different transmit powers to different DUs.[2]

For OMA transmission, the transmission time slot for each BS is further divided into smaller sub-slots for transmissions to the individual DUs as illustrated in Fig. 2(a). For NOMA, every DU is allocated the whole time for transmission as depicted in Fig. 2(b).

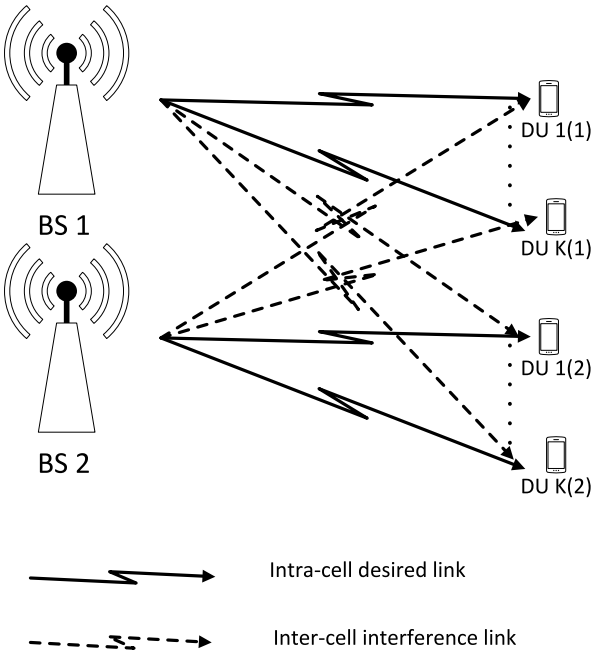

FIGURE 1. Multi-cell System model comprising of two BSs and multiple DUs.

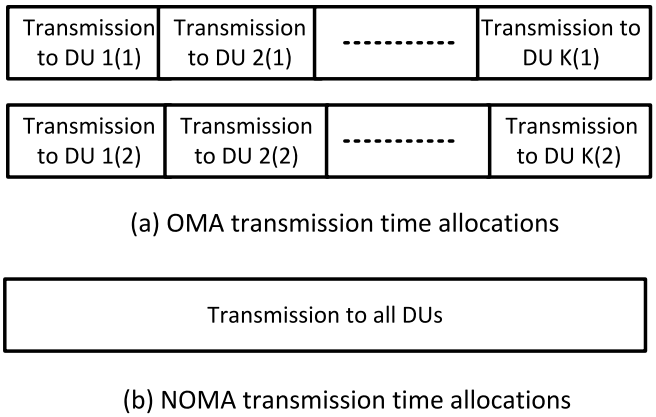

FIGURE 2. Time allocation for OMA and NOMA transmissions.

2. In the rest of this paper, for ease of exposition NOMA explicitly refers to power-domain NOMA with SIC at the receivers.

A. ENERGY CONSUMPTION FOR COMPRESSION

Following an approach similar to [48], [49], we model the effect of compression on the energy consumption with the help of compression ratio, which is defined as the ratio between the sizes of input data to the compressor and output data of the compressor. Assuming that $\beta_m \geq 1$ represents the compression ratio of the m-th BS, and if L_m^{in} denotes the total bits that are fed to the compressor within the m-th BS, then the number of output bits will be $L_m^{out} = \frac{L_m^{in}}{\beta_m}$. Moreover, the total number of compressed bits for m-th BS are given by

$$L_m = L_m^{in} - L_m^{out} = L_m^{in} - \frac{L_m^{in}}{\beta_m}. \tag{1}$$

It is reasonable to assume that a higher compression ratio will require more processing. The amount of processing can be expressed in terms of the number of central processing unit (CPU) cycles needed to carry out the computation process for performing compression. The number of CPU cycles for compressing single bit data with a compression ratio β can be expressed as [48], [49]

$$C = e^{\beta\epsilon} - e^{\epsilon}, \tag{2}$$

where ϵ depends on the compression technique. Assuming that the energy consumed for one CPU cycle is ϱ, the total energy consumed for compression within the m-th BS can then be written as [48], [49]

$$E_c = L_m^{in} C \varrho. \tag{3}$$

Now using the expression for C and the relationship between L_m^{in}, β_m and L_m as given in (1), we can write the consumed energy for compression for m-th BS in terms of compressed bits L_m as

$$E_c^{L_m} = L_m^{in}\left(e^{\frac{L_m^{in}}{L_m^{in}-L_m}\epsilon} - e^{\epsilon}\right)\varrho. \tag{4}$$

Remark 1: In our current work, we focus only on the energy consumed at the BS. The motivation behind this assumption is that the BS has to account for transmission energy and compression energy for all the DUs. On the contrary, in our system model each DU only decompresses its own desired information. Therefore, the energy consumed at each individual DU is much smaller than the compression energy consumed at the BS. There are various existing works which support this assumption. Specifically, the existing works [50], [51], [52] observed following two facts about the decompression energy.

- *F1:* Decompression energy consumption is comparatively much smaller than the compression energy consumption [50, Fig. 1(a)], [51].
- *F2:* Decompression energy consumption is stable/constant over a wide range of compression ratios [52, Figs. 6 and 7].

Essentially, **F1** means that the decompression power consumption will have negligible effect on the overall energy consumption and **F2** means that the solution approach used in this paper is still applicable when decompression energy is taken into account since it will appear as a constant term in the objective function of the optimization problems. Therefore, in order to simplify the notation we ignore the decompression energy in the rest of the paper.

B. ENERGY CONSUMPTION FOR TRANSMISSION

In the following, we represent the k-th DU of m-th BS by $k(m)$. Then, the channel gain and distance between the r-th BS and the $k(m)$-th DU are denoted by $|h_{k,m,r}|^2$ and $d_{k,m,r}$, respectively. We assume $|h_{k,m,r}|^2$ follows exponential distribution with parameter $\Lambda_{k,m,r}$, where $\Lambda_{k,m,r} = d_{k,m,r}^n$ and n is the path loss exponent. Without loss of generality, we assume $\Lambda_{1,m,m} \geq \Lambda_{2,m,m} \cdots \geq \Lambda_{K(m),m,m}$ $\forall\ m \in \{1, 2, \ldots, M\}$. We consider two types of downlink transmissions, namely: power-domain NOMA and OMA. First, we describe NOMA transmission scheme and then we provide details of OMA transmission scheme.

1) NOMA TRANSMISSION

For NOMA transmission the received signal at the $k(m)$-th DU can be written as

$$y_{k,m}^{NOMA} = \sum_{r=1}^{M} h_{k,m,r} \sum_{j=1}^{K(r)} \sqrt{P_{j,r}^{L_{j,r}^t}}\, a_{j,r} + \omega_{k,m}, \tag{5}$$

where $P_{j,r}^{L_{j,r}^t}$ is the power allocated to $j(r)$-th DU as a function of bits transmitted to $j(r)$-th DU which are denoted by $L_{j,r}^t$, $a_{j,r}$ is the symbol destined for $j(r)$-th DU and $\omega_{k,m}$ is the additive white Gaussian noise at the $k(m)$-th DU with zero mean and variance $\sigma_{k,m}^2$. Moreover, we assume that all the DUs employ SIC for decoding, where a DU at the higher decoding order decodes the information of all the DUs with lower decoding order and subsequently subtracts it from the received signal to mitigate the interference caused by all the lower decoding order DUs. Hence, all the receivers employ a specific decoding order and $\chi_m(j)$ denotes the decoding order of the $j(m)$-th DU during the SIC. We denote $R_{\chi_m(l)}^{\chi_m(k)}$ to be the data rate for user $\chi_m(k)$ for decoding user $\chi_m(l)$'s signal with $l(m) \leq k(m)$. According to the principal of perfect[3] SIC, we can write $R_{\chi_m(l)}^{\chi_m(k)}$ as shown in (6) at the bottom of next page.

Based on the above assumptions, we provide the following lemma regarding the OP, $\mathbb{P}_{out}^{\chi_m(k),L_{\chi_m(k),m}^t}$, of the $\chi_m(k)$-th DU.

Lemma 1: The OP $\mathbb{P}_{out}^{\chi_m(k),L_{\chi_m(k),m}^t}$ is given by (7) shown at the bottom of next page.

Proof: First, we note that the PDF of $|h_{\chi_m(k),m,r}|^2$ is given as $f_{|h_{\chi_m(k),m,r}|^2}(x) = \Lambda_{\chi_m(k),m,r} e^{-\Lambda_{\chi_m(k),m,r}x}$ and the corresponding complementary cumulative distribution function (CCDF) is given as $Pr(|h_{\chi_m(k),m,r}|^2 \geq x) = e^{-\Lambda_{\chi_m(k),m,r}x}$. Second, we note that the SINR corresponding to the signal of $\chi_m(l)$-th DU at the $\chi_m(k)$-th DU, with SIC decoding, is given as (8) at the bottom of next page. Then, the event

3. The case of imperfect SIC is considered in Section IV-B.

$R^{\chi_m(k)}_{\chi_m(l)} \geq L^t_{\chi_m(l),m}$ can be simplified as (9) shown at the bottom of the page.

Third, we note that in SIC decoding the $\chi_m(k)$-th DU needs to decode all the $\chi_m(l)$ DUs with $\chi_m(l) \leq \chi_m(k)$ to successfully decode its own information. Therefore, the success probability for the $\chi(k)$-th DU, $Pr(R^{\chi(k)}_{\chi(1)} \geq L^t_{\chi(1)}, \ldots, R^{\chi(k)}_{\chi(k)} \geq L^t_{\chi(k)})$, is given as (10) shown at the bottom of the page. It is well know that if a random variable $\mathbf{x}$ has CCDF $F_{\mathbf{x}}(x)$, then the probability $Pr(\cap_{i\in\{1,\ldots,K\}}\mathbf{x} \geq c_i) = F_{\mathbf{x}}(\max_{i\in\{1,\ldots,K\}} c_i)$, where c_i's are constants. Using this fact and the CCDF of $|h_{\chi_m(k),m,m}|^2$, we can further simplify the success probability for DU $\chi_x(k)$ as shown in (11) at the bottom of the page.

Finally using the definition of probability for complementary events, we arrive at the result presented in equation (7). ■

Note that the OP in (7) for the SIC reception can only be smaller than 1 if we have

$$P^{L^t_{\chi_m(l),m}}_{\chi_m(l),m} - \left(2^{L^t_{\chi_m(l),m}} - 1\right) \sum_{j=l+1}^{K} P^{L^t_{\chi_m(j),m}}_{\chi_m(j),m} > 0.$$

2) OMA TRANSMISSION

For OMA transmission, each of the BS divides the whole transmission time slot into $K(m)$ sub-slots and the received signal at the $k(m)$-th DU during k-th sub-slot is given as

$$y^{OMA}_k = h_{k,m,m}\sqrt{P^{L^t_{k,m}}_{k,m}}a_{k,m} + \sum_{r=,r\neq m}^{M} h_{k,m,r}\sum_{j=1}^{K(r)}\sqrt{P^{L^t_{j,r}}_{j,r}}\hat{a}_{j,r} + \omega_{k,m}, \tag{12}$$

where $\hat{a}_{j,r} = 0$ if time allocation for $j(r)$-th DU does not coincide with the time allocation for $k(m)$-th DU, else $\hat{a}_{j,r} = a_{j,r}$. Then, assuming that the k-th sub-slot has a duration of t^t_k seconds the transmitted bits to the k-th DU can be written as

$$R^{OMA}_{k,m} = t^t_{k,m}\log_2\left(1 + \frac{|h_{k,m,m}|^2 P^{L^t_{k,m}}_{k,m}}{u_{k,m} + \sigma^2_{k,m}}\right), \tag{13}$$

where

$$u_{k,m} = \sum_{r=1,r\neq m}^{M} |h_{k,m,r}|^2 \sum_{j=1}^{K(r)} P^{L^t_{j,r}}_{j,r}|\hat{a}_{j,r}|^2.$$

The OP can then be written as

$$\mathbb{P}^{k,L^t_k}_{out} = Pr(R^{OMA}_k \leq L^t_k). \tag{14}$$

Remark 2: Although the transmission circuitry also consumes energy, this energy is static [53], [54] and appears as a constant summation term in the objective function of the optimization problems considered in this paper. Hence, it does not affect the solution of the optimization problems. Therefore, we do not consider this static energy in an attempt to simplify the notation.

III. OPTIMIZATION PROBLEMS FORMULATION

In this section, we formulate the optimization problems. The objective of the proposed optimization problems is to minimize the total energy consumption while guaranteeing the QoS constraints for the DUs. First, we write the optimization problem for NOMA, then we present the optimization problem for OMA.

$$R^{\chi_m(k)}_{\chi_m(l)} = \log_2\left(1 + \frac{|h_{\chi_m(k),m,m}|^2 P^{L^t_{\chi_m(l),m}}_{\chi_m(l),m}}{|h_{\chi_m(k),m,m}|^2 \sum_{j=l+1}^{K(m)} P^{L^t_{\chi_m(j),m}}_{\chi_m(j),m} + |h_{\chi_m(k),m,r}|^2 \sum_{j=1}^{K(r)} P^{L^t_{\chi_r(j),r}}_{\chi_r(j),r} + \sigma^2_{\chi_m(k),m}}\right). \tag{6}$$

$$\mathbb{P}^{\chi(k),L^t_{\chi(k)}}_{out} = 1 - e^{-\max_{i=1\ldots k}\frac{\sigma^2_{\chi(k)}\Lambda_{\chi(k)}(2^{L^t_{\chi(i)}}-1)}{P^{L^t_{\chi(i)}}_{\chi(i)} - (2^{L^t_{\chi(i)}}-1)\sum_{j=i+1}^{K} P^{L^t_{\chi(j)}}_{\chi(j)}}}. \tag{7}$$

$$SINR^{\chi_m(k)}_{\chi_m(l)} = \frac{|h_{\chi_m(k),m,m}|^2 P^{L^t_{\chi_m(l),m}}_{\chi_m(l),m}}{|h_{\chi_m(k),m,m}|^2 \sum_{j=l+1}^{K(m)} P^{L^t_{\chi_m(j),m}}_{\chi_m(j),m} + |h_{\chi_m(k),m,r}|^2 \sum_{j=1}^{K(r)} P^{L^t_{\chi_r(j),r}}_{\chi_r(j),r} + \sigma^2_{\chi_m(k),m}}, \tag{8}$$

$$R^{\chi_m(k)}_{\chi_m(l)} \geq L^t_{\chi_m(l),m} \Rightarrow |h_{\chi_m(k),m,m}|^2 \geq \frac{\left(|h_{\chi_m(k),m,r}|^2 \sum_{j=1}^{K(r)} P^{L^t_{\chi_r(j),r}}_{\chi_r(j),r} + \sigma^2_{\chi_m(k),m}\right)\left(2^{L^t_{\chi_m(l),m}} - 1\right)}{P^{L^t_{\chi_m(l),m}}_{\chi_m(l),m} - \left(2^{L^t_{\chi(i)}} - 1\right)\sum_{j=i+1}^{K(m)} P^{L^t_{\chi_m(j),m}}_{\chi_m(j),m}}. \tag{9}$$

$$Pr\left(\bigcap_{l\in\{1,\cdots,k\}} |h_{\chi_m(k),m,m}|^2 \geq \frac{\left(|h_{\chi_m(k),m,r}|^2 \sum_{j=1}^{K(r)} P^{L^t_{\chi_r(j),r}}_{\chi_r(j),r} + \sigma^2_{\chi_m(k),m}\right)\left(2^{L^t_{\chi_m(l),m}} - 1\right)}{P^{L^t_{\chi_m(l),m}}_{\chi_m(l),m} - \left(2^{L^t_{\chi_m(l),m}} - 1\right)\sum_{j=l+1}^{K} P^{L^t_{\chi_m(j),m}}_{\chi_m(j),m}}\right). \tag{10}$$

$$Pr\left(R^{\chi(k)}_{\chi(1)} \geq L^t_{\chi(1)}, \ldots, R^{\chi(k)}_{\chi(k)} \geq L^t_{\chi(k)}\right) = e^{-\max_{i=1\ldots k}\frac{\left(|h_{\chi_m(k),m,r}|^2 \sum_{j=1}^{K(r)} P^{L^t_{\chi_r(j),r}}_{\chi_r(j),r} + \sigma^2_{\chi_m(k),m}\right)\left(2^{L^t_{\chi_m(l),m}} - 1\right)}{P^{L^t_{\chi_m(l),m}}_{\chi_m(l),m} - \left(2^{L^t_{\chi_m(l),m}} - 1\right)\sum_{j=l+1}^{K} P^{L^t_{\chi_m(j),m}}_{\chi_m(j),m}}}. \tag{11}$$

A. OPTIMIZATION PROBLEM FOR NOMA

Mathematically, the optimization problem for NOMA downlink scenario can be written as follows:

$$\mathbf{P1}: \min \sum_{m=1}^{M} E_c^{\mathscr{L}_m} + t_t \sum_{m=1}^{M}\sum_{k=1}^{K(m)} P_{\chi_m(k),m}^{L^t_{\chi_m(k),m}} \tag{15}$$

$$\text{s.t.} \quad 0 \le P_{\chi_m(k),m}^{L^t_{\chi_m k,m}}, \tag{16}$$

$$\Gamma_{\chi_m(k),m}^{L^t_{\chi_m(k),m}} \sum_{j=k+1}^{K} P_{\chi_m(j),m}^{L^t_{\chi_m(j),m}} < P_{\chi_m(k),m}^{L^t_{\chi_m(k),m}}, \tag{17}$$

$$\mathbb{P}_{out}^{\chi_m(k),L^t_{\chi_m(k),m}} \le \theta_{\chi_m(k)}, \tag{18}$$

$$L^{min} \le L^t_{\chi_m(k),m}, \tag{19}$$

$$\chi_m \in \Xi, \tag{20}$$

$$\sum_{k=1}^{K(m)} L_{\chi_m(k),m} - L^t_{\chi_m(k),m} \le \mathscr{L}_m, \tag{21}$$

$$L_{\chi_m(k),m} - L^t_{\chi_m(k),m} \ge 0, \tag{22}$$

where Ξ is the set of all possible decoding orders, $L_{\chi_m(k),m}$ is the number of bits for DU $\chi_m(k)$, $L^t_{\chi_m(k),m} = L_{\chi_m(k),m} - L^c_{\chi_m(k),m}$, $\Gamma_{\chi_m(k),m}^{L^t_{\chi_m(k),m}} = 2^{L^t_{\chi_m(k),m}} - 1$ and L^{min} is the minimum rate requirement of user $\chi_m(k)$.

In **P1**, the objective is the sum of compression energy and the transmission energy. The compression energy is dependent on the amount of compression performed, which is indicated by $\mathscr{L}_m$. The transmission energy is dependent on the transmission bits which are indicated by $L^t_{\chi_m(k),m}, \forall k \in \{1,\ldots,K\}$. The constraints (16) represent the non-negativity of consumed powers during transmission phases. The SIC based decoding constraint is represented by (17). The QoS requirement on the OP for individual DUs is represented by (18), where $\mathbb{P}_{out}^{\chi_m(k),L^t_{\chi_m(k),m}}$ denotes the OP for DU $\chi_m(k)$ at transmission data rate $L^t_{\chi_m(k),m}$. The constraint on the minimum number of transmitted bits for DU $\chi_m(k)$ is represented by (19). The decoding order constraint is given by (20). The constraint (21) ensures that the total number of compressed bits, $\mathscr{L}_m$, should be greater than the sum of compressed bits of individual DUs. Finally, (22) guarantees that the transmitted bits are smaller than the maximum transmitted bits budget in a time slot.

The optimization problem **P1** is a non-convex optimization problem and is difficult to solve. The non-convexity arise due to the decoding order constraint of the problem. Although **P1** is difficult to solve, an efficient solution for problem **P1** will be presented in Section IV-A for single-cell scenario and in Section V-A for multi-cell scenario.

B. OPTIMIZATION PROBLEM FOR OMA

The optimization problem for OMA downlink scenario can be written as follows:

$$\mathbf{P2}: \min \sum_{m=1}^{M} E_c^{\mathscr{L}_m} + \sum_{m=1}^{M}\sum_{k=1}^{K(m)} t^t_{k,m} P_{k,m}^{L^t_{k,m}} \tag{23}$$

$$\text{s.t.} \quad 0 \le P_{k,m}^{L^t_{k,m}}, \tag{24}$$

$$\mathbb{P}_{out}^{k(m),L^t_{k,m}} \le \theta_{k,m}, \tag{25}$$

$$L^{min} \le L^t_{k,m}, \tag{26}$$

$$\sum_{k=1}^{K(m)} L_{k,m} - L^t_{k,m} \le \mathscr{L}_m, \tag{27}$$

$$L_{k,m} - L^t_{k,m} \ge 0, \tag{28}$$

$$0 \le t^t_{k,m}, \tag{29}$$

$$\sum_{k=1}^{K(m)} t^t_{k,m} \le t_t, \tag{30}$$

where $t^t_{k,m}$ is the transmission time allocated for $k(m)$-th DU.

In **P2**, the objective function is different from **P1** in the sense of transmission energy. For OMA, we have orthogonal time allocations and therefore the total transmission energy is the product of DUs time allocations and power allocations. The constraint (24) guarantee the non-negativity of transmit powers. The constraints on the OPs of DUs are enforced by (25). The constraint on the minimum number of transmitted bits for user $k(m)$ is represented by (26). The constraint (27) ensures that the total number of compressed bits, $\mathscr{L}_m$, are greater than the sum of compressed bits of individual DUs. The constraint (28) guarantees that the transmitted bits are smaller than the maximum transmitted bits budget in a time slot. The constraints on the time allocations are given by (29) and (30).

It is clear that **P2** is non-convex. The non-convexity arises due to the products of optimization variables in the objective function. Although, exhaustive search can be employed to obtain the solution of **P2**, the computational complexity of such an approach is very high. Although **P2** is difficult to solve, an efficient solution for problem **P2** will be presented in Section IV-C for single-cell scenario and in Section V-B for the multi-cell scenario.

IV. PROPOSED SOLUTION FOR OVERALL ENERGY CONSUMPTION MINIMIZATION IN SINGLE CELL SCENARIO

In order to solve the above optimization problems eventually for multi-cell scenario, first we study the single-cell scenario in this section. Then, we use the obtained insights to devise efficient algorithms for solving the complete multi-cell problem in Section V.

In this section, in order to simplify the notation, we drop the subscript m from all notations. Also, a comprehensive list of the system parameters used in the single-cell scenario is provided in Table 1. In the following, first we present globally optimal solutions for **P1**, and **P2** for fixed value of $\mathscr{L}$. Then, we use linear search over $\mathscr{L}$ for finding the optimal value of $\mathscr{L}$. Note that the linear search for $\mathscr{L}$ should be performed over $[0, \sum_{k=1}^{K} L_k - L^{min}]$. This is due to the fact that the minimum transmission rate for the k-th DU must be greater than L^{min} according to the QoS constraint. For ease of exposition, this section is divided into four subsections.

TABLE 1. Summary of notations used for single-cell scenario.

Parameter	Value
k-th user channel	h_k
Path loss exponent	n
distance between k-th DU and BS	d_k
transmission bits for k-th DU after compression	L_k^t
transmission bits for k-th DU without compression	L_k
compressed bit for the k-th DU	L_k^c
minimum data rate requirement of each DU	L^{min}
transmit symbol for the k-th DU	a_k
transmit power for k-th DU for L_k^t transmission bits	$P_k^{L_k^t}$
noise at the k-th DU	ω_k
noise power at the k-th DU	σ_k^2
outage probability of k-th DU	$\mathbb{P}_{out}^{k,L_k^t}$
outage probability threshold for k-th DU	θ_k
transmit time in NOMA scheme	t^t
transmit time for k-th DU in OMA scheme	t_k^t
total number of DUs	K
CPU cycles for processing one bit	C
energy consumed for one CPU cycle	ϱ

Sections IV-A and IV-B discuss the solution methodology for problems **P1** with perfect SIC, imperfect SIC, respectively while Section IV-C discusses the solution approach for **P2**. Finally, Section IV-D summarizes the proposed optimization algorithms.

A. SOLVING P1 FOR FIXED VALUE OF $\mathscr{L}$

For a fixed feasible value of $\mathscr{L} = \mathrm{L}$, we use the following steps for finding the optimal solution of problem **P1**:

- S1: First, solve for feasible set of transmission rates, $L_{\chi(k)}^t$, and obtain the closed-form expressions for optimal transmit powers.
- S2: Then, solve the optimization problem based on the closed-form expressions obtained in step S1 under the transmission rate constraints.

1) SOLVING P1 FOR A FIXED FEASIBLE SET OF TRANSMISSION RATES

For a fixed feasible set of transmission rates with a given $\mathscr{L} = \mathrm{L}$, the problem **P1** can be written as

$$\mathbf{P3}: \min_{\chi, P_{\chi(k)}^{L_{\chi(k)}^t}} \sum_{k=1}^{K} P_{\chi(k)}^{L_{\chi(k)}^t} \tag{31}$$

$$\text{s.t.} \quad 0 \le P_{\chi(k)}^{L_{\chi(k)}^t}, \tag{32}$$

$$\Gamma_{\chi(k)}^{L_{\chi(k)}^t} \sum_{j=k+1}^{K} P_{\chi(j)}^{L_{\chi(j)}^t} < P_{\chi(k)}^{L_{\chi(k)}^t}, \tag{33}$$

$$\mathbb{P}_{out}^{\chi(k),L_{\chi(k)}^t} \le \theta_{\chi(k)}, \tag{34}$$

$$\chi \in \Xi. \tag{35}$$

The main difficulty in solving **P3** lies in the decoding order constraint. With the help of Lemma 1, the OP constraint can be reformulated as follows:

$$\min_{i=1,\ldots,k} \frac{P_{\chi(i)}^{L_{\chi(i)}^t} - (2^{L_{\chi(i)}^t} - 1) \sum_{j=i+1}^{K} P_{\chi(j)}^{L_{\chi(j)}^t}}{2^{L_{\chi(i)}^t} - 1} \ge \frac{\Lambda_{\chi(k)} \sigma_{\chi(k)}^2}{\log\left(\frac{1}{1-\theta_{\chi(k)}}\right)}. \tag{36}$$

Before proceeding further, we provide following lemma which facilitates the later derivations.

Lemma 2: Assuming $s_{\chi(i)}^{L_{\chi(i)}^t} = P_{\chi(i)}^{L_{\chi(i)}^t} - (2^{L_{\chi(i)}^t} - 1) \sum_{j=i+1}^{K} P_{\chi(j)}^{L_{\chi(j)}^t}$ for $i \in \{1, \ldots, K\}$. We have the following relationships between $s_{\chi(i)}^{L_{\chi(i)}^t}$ and $P_{\chi(i)}^{L_{\chi(i)}^t}$.

$$P_{\chi(i)}^{L_{\chi(i)}^t} = s_{\chi(i)}^{L_{\chi(i)}^t} + (2^{L_{\chi(i)}^t} - 1) \sum_{j=i+1}^{K} \prod_{k=i+1}^{j-1} 2^{L_{\chi(k)}^t} s_{\chi(j)}^{L_{\chi(j)}^t}, \tag{37}$$

and

$$\sum_{k=1}^{K} P_{\chi(k)}^{L_{\chi(k)}^t} = \sum_{k=1}^{K} \zeta_{\chi(k)}^{L_{\chi(k)}^t} s_{\chi(k)}^{L_{\chi(k)}^t}, \tag{38}$$

where

$$\zeta_{\chi(k)}^{L_{\chi(k)}^t} = \begin{cases} 1, & \chi(k) = 1 \\ \prod_{i=1}^{k-1} 2^{L_{\chi(i)}^t}, & \chi(k) = 2, \ldots, K. \end{cases} \tag{39}$$

Proof: From the definition of $s_{\chi(k)}^{L_{\chi(k)}^t}$, we can write

$$P_{\chi(i)}^{L_{\chi(i)}^t} = s_{\chi(i)}^{L_{\chi(i)}^t} + (2^{L_{\chi(i)}^t} - 1) \sum_{j=i+1}^{K} P_{\chi(j)}^{L_{\chi(j)}^t}. \tag{40}$$

Also, from (40) we can derive the following relation for $\sum_{k=i+1}^{K} P_{\chi(k)}^{L_{\chi(k)}^t}$

$$\sum_{k=i+1}^{K} P_{\chi(k)}^{L_{\chi(k)}^t} = s_{\chi(i+1)}^{L_{\chi(i+1)}^t} + 2^{L_{\chi(i+1)}^t} \sum_{k=i+2}^{K} P_{\chi(k)}^{L_{\chi(k)}^t}, \tag{41}$$

$$= s_{\chi(i+1)}^{L_{\chi(i+1)}^t} + \sum_{k=i+2}^{K} \prod_{j=i+1}^{k-1} 2^{L_{\chi(j)}^t} s_{\chi(k)}^{L_{\chi(k)}^t}. \tag{42}$$

Next, using the definition of $\zeta_{\chi(k)}^{L_{\chi(k)}^t}$ provided in (39), we can write (42) as

$$\sum_{k=1}^{K} P_{\chi(k)}^{L_{\chi(k)}^t} = \sum_{k=1}^{K} \zeta_{\chi(k)}^{L_{\chi(k)}^t} s_{\chi(k)}^{L_{\chi(k)}^t}. \tag{43}$$

This completes the proof. ■

Then, using the result of Lemma 2 and (36), we can reformulate **P3** into following equivalent form

$$\mathbf{P3-Eq}: \min_{\chi, s_{\chi(k)}^{L_{\chi(k)}^t}} \sum_{k=1}^{K} \zeta_{\chi(k)}^{L_{\chi(k)}^t} s_{\chi(k)}^{L_{\chi(k)}^t} \tag{44}$$

$$\text{s.t.} \quad 0 < s_{\chi(k)}^{L_{\chi(k)}^t}, \tag{45}$$

$$\chi \in \Xi, \tag{46}$$

$$\delta_{\chi(k)} \leq \min_{i=1,\ldots,k} \frac{s_{\chi(i)}^{L_{\chi(i)}^t}}{2^{L_{\chi(i)}^t} - 1}, \tag{47}$$

where $\delta_{\chi(k)} = \frac{\Lambda_{\chi(k)}\sigma_{\chi(k)}^2}{\log(\frac{1}{1-\theta_{\chi(k)}})}$ is termed as the path loss factor (PLF) for k-th DU in the rest of the paper. Still the decoding order constraint causes difficulty in finding the solution for problem **P3-Eq**. To circumvent this issue, the following lemma provides the optimal decoding order for **P3-Eq**.

Lemma 3: The optimal decoding order, denoted by $\chi*$, for problem **P3-Eq** has the following property.

$$\delta_{\chi*(1)} > \delta_{\chi*(2)} > \cdots > \delta_{\chi*(K)}. \tag{48}$$

Proof: First, we define κ such that

$$\frac{s_{\chi(\kappa)}^{L_{\chi(\kappa)}^t}}{2^{L_{\chi(\kappa)}^t} - 1} = \min_{i\in\{1,2,\ldots,k\}} \frac{s_{\chi(k)}^{L_{\chi(k)}^t}}{2^{L_{\chi(k)}^t} - 1}. \tag{49}$$

With the help of (49), the outage constraints for user k and $k+1$ can be written as

$$\frac{s_{\chi(\kappa)}^{L_{\chi(\kappa)}^t}}{2^{L_{\chi(\kappa)}^t} - 1} \geq \delta_{\chi(k)}, \tag{50}$$

$$\min\left\{\frac{s_{\chi(\kappa)}^{L_{\chi(\kappa)}^t}}{2^{L_{\chi(\kappa)}^t} - 1}, \frac{s_{\chi(k+1)}^{L_{\chi(k+1)}^t}}{2^{L_{\chi(k+1)}^t} - 1}\right\} \geq \delta_{\chi(k+1)}. \tag{51}$$

It is clear from (50), (51) that if $\delta_{\chi(k)} \leq \delta_{\chi(k+1)}$, then by using another decoding order χ', where χ' is defined such that

$$\begin{aligned} \chi'(1) = \chi(1), \ldots, \chi'(k-1) = \chi(k-1), \\ \chi'(k) = \chi(k+1), \chi'(k+1) = \chi(k), \\ \chi'(k+2) = \chi(k+2), \ldots, \chi'(K) = \chi(K), \end{aligned} \tag{52}$$

the value of $\frac{s_{\chi(\kappa)}^{L_{\chi(\kappa)}^t}}{2^{L_{\chi(\kappa)}^t}-1}$ will remain same however $\frac{s_{\chi(k+1)}^{L_{\chi(k+1)}^t}}{2^{L_{\chi(k+1)}^t}-1}$ is non-increasing. Hence, by using the decoding order χ' instead of χ will either decrease the objective function of **P3-Eq** or will keep it equal to the objective function achieved by χ. This procedure can be repeated until (48) is valid. Therefore, by successively exchanging the decoding order of adjacent users until (48) is valid will result in reduction of the objective function. This completes the proof. ■

The main insight behind this ordering is that the relatively worse DUs should be decoded first with the minimum possible power allocated for their corresponding transmissions. This results in smaller power needed for transmitting to the relatively better DUs which should be decoded later, since the power allocated to the DUs which are decoded first must be greater than the powers allocated to the DUs decoded later. Thus, resulting in overall reduction of the total transmit power.

For ease of notation, in the rest of *this section*, without loss of generality, we assume that $\chi^*(1) = 1, \chi^*(2) = 2, \ldots, \chi^*(K) = K$. This means, in the rest of *this section*, δ_k's are sorted as

$$\delta_1 > \delta_2 > \cdots > \delta_K. \tag{53}$$

With the help of Lemma 3 and assumption (53), the optimization problem **P3-Eq** can be simplified as

$$\textbf{P3} - \textbf{Eq} - \textbf{Sim}: \min_{s_k^{L_k^t}} \sum_{k=1}^{K} \zeta_k^{L_k^t} s_k^{L_k^t} \tag{54}$$

$$\text{s.t.} \quad 0 < s_k^{L_k^t}, \tag{55}$$

$$\delta_k \leq \min_{i=1,\ldots,k} \frac{s_i^{L_i^t}}{2^{L_i^t} - 1}. \tag{56}$$

Then, the following lemma provides the optimal transmit powers for **P3-Eq-Sim**.

Lemma 4: The optimal transmit power for $k \in \{1, 2, \ldots, K\}$-th user is given as

$$P_k^{L_k^t *} = (2^{L_k^t} - 1)\left(\delta_k + \sum_{i=k+1}^{K} (2^{L_i^t} - 1)\delta_i 2^{\sum_{j=k+1}^{i-1} L_j^t}\right). \tag{57}$$

Proof: With the help of induction, it can be easily shown that the constraint (56) is equivalent to

$$\frac{s_k^{L_k^t}}{2^{L_k^t} - 1} \geq \delta_k, \tag{58}$$

$$\frac{s_k^{L_k^t}}{2^{L_k^t} - 1} \geq \delta_{k+1}, \tag{59}$$

$$\vdots$$

$$\frac{s_k^{L_k^t}}{2^{L_k^t} - 1} \geq \delta_K. \tag{60}$$

Using (52), we can further simplify (58)-(60) as

$$s_k^{L_k^t} \geq \delta_k(2^{L_k^t} - 1). \tag{61}$$

It is clear that the objective function of **P3-Eq-Sim** is increasing with $s_k^{L_k^t}$. Thus, the optimal value of $s_k^{L_k^t}$ is given by the lower bound provided in (61). Then, using the relationship between $s_k^{L_k^t}$ and $P_k^{L_k^t}$ and after some mathematical manipulations, we can arrive at the result provided in (57). ■

2) SOLVING P1 OVER TRANSMISSION RATE CONSTRAINTS

By using the results of Section IV-A1, the optimization problem **P1** for a given value of $\mathscr{L} = L$ can be simplified as

P3-Sim:

$$\min_{L_k^t} \sum_{k=1}^{K}\left(2^{L_k^t} - 1\right)\left(\delta_k + \sum_{i=k+1}^{K}\left(2^{L_i^t} - 1\right)\delta_i 2^{\sum_{j=k+1}^{i-1} L_j^t}\right) \tag{62}$$

$$\text{s.t.} \quad L^{min} \leq L_k^t, \tag{63}$$

$$\sum_{k=1}^{K} L_k - L_k^t \leq L, \tag{64}$$

$$L_k - L_k^t \geq 0. \tag{65}$$

We have following theorem for problem **P3-Sim**.

Theorem 1: The problem **P3-Sim** has following properties.

- A1: **P3-Sim** is a convex optimization problem.
- A2: If for $\hat{k}$-th DU both the constraints (63) and (65) are inactive, then for $(\hat{k}+1)$-th DU, the constraint (63) is inactive and constraint (65) is active. Furthermore, for $(\hat{k}-1)$-th DU the constraint (63) must be active and the constraint (65) must be inactive.
- A3: If $\mathscr{A}$ denote the set of DUs for which both constraints (63) and (65) are inactive simultaneously, then $|\mathscr{A}| \leq 1$, where $|\mathscr{A}|$ denotes the cardinality of $\mathscr{A}$.

Proof: First, we observe that all the constraints are linear. Moreover, through the vector composition rules stated in [55, p. 86], it can be shown that the objective function is a non-negative weighted sum of convex functions. Therefore, property A1 is proved.

Since **P3-Sim** is a convex optimization problem, we can use the KKT conditions to obtain its solution. The Lagrangian of **P3-Sim** can be written as

$$\begin{aligned}\mathcal{G}(\lambda_k, \nu_k, \rho, L_k^t) &= \sum_{k=1}^{K} \lambda_k (L_k^{min} - L_k^t) + \sum_{k=1}^{K} \nu_k (L_k^t - L_k) \\ &+ \sum_{k=1}^{K} (2^{L_k^t} - 1)(\delta_k + \sum_{i=k+1}^{K} (2^{L_i^t} - 1)\delta_i 2^{\sum_{j=k+1}^{i-1} L_j^t}) \\ &+ \rho(\sum_{k=1}^{K} L_k - L_k^t - L).\end{aligned} \tag{66}$$

In (66), we assume λ_k to be the dual variable associated with the k-th user minimum rate constraint, ν_k to be the dual variable associated with k-th constraint in (65), and ρ to be the dual variable associated with constraint (64). Then, KKT optimality conditions can be written as

$$\frac{\partial \mathcal{G}(\lambda_k^*, \nu_k^*, \rho^*, L_k^{t*})}{\partial L_k^t} = 0, \tag{67}$$

$$\lambda_k^* \left(L^{min} - L_k^{t*}\right) = 0, \tag{68}$$

$$\nu_k^* \left(L_k^{t*} - L_k\right) = 0 \tag{69}$$

$$\rho^* \left(\sum_{k=1}^{K} L_k - L_k^{t*} - L\right) = 0 \tag{70}$$

$$\lambda_k^* \geq 0, \nu_k^* \geq 0, \rho^* \geq 0. \tag{71}$$

After taking the derivative of the Lagrangian $\mathcal{G}(\lambda_k, \nu_k, \rho, L_k^t)$ with respect to L_k^t and equating it to zero, we can write

$$\rho^* = 2^{\sum_{i=1}^{k} L_i^{t*}} \delta_k + \sum_{j=k+1}^{K} 2^{\sum_{i=1}^{j-1} L_i^{t*}} \delta_j (2^{L_j^{t*}} - 1) - \lambda_k^* + \nu_k^*. \tag{72}$$

For ρ^* there are two possibilities: either $\rho^* = 0$ or $\rho^* > 0$. We consider these possibilities in the following.

Case i): If $\rho^* = 0$, then it is clear that all the λ_k's are positive. Now using the complementary slackness conditions (68), it can be easily shown that all the minimum rate constraints must be active. Therefore, there is no such DU for which both the constraints (63) and (65) are inactive. Hence, property A2 does not apply for this particular case. Moreover, for this particular case $|\mathscr{A}| = 0$. Thus, property A3 is also proved for this special case.

Case ii): If $\rho^* > 0$, then after some mathematical manipulations, we can arrange the equations (72) as follows:

$$2^{\sum_{i=1}^{k} L_i^t} (\delta_k - \delta_{k+1}) = \lambda_k^* - \nu_k^* - (\lambda_{k+1}^* - \nu_{k+1}^*). \tag{73}$$

Now using the fact that $\delta_k > \delta_{k+1}$, we conclude that

$$\lambda_k^* - \nu_k^* > \lambda_{k+1}^* - \nu_{k+1}^*, \tag{74}$$

is true for all $k \in \{1, \ldots, K-1\}$. Assume that for $\hat{k}$-th user both constraints (63) and (65) are inactive. Then, due to complementary slackness conditions both $\lambda_{\hat{k}}^*$ and $\nu_{\hat{k}}^*$ must be zero. Therefore, (74) can be true only if $\lambda_{\hat{k}+1}^* < \nu_{\hat{k}+1}^*$. However, if $\nu_{\hat{k}+1}^*$ is positive, then constraint (65) for $(\hat{k}+1)$-th user must be active. This also leads to the conclusion that $(\hat{k}+1)$-th constraint in (63) is inactive. This proves the first part stated in property A2.

Now we consider the second statement made in property A2. From (74) and the fact that $\lambda_{\hat{k}}^* = \nu_{\hat{k}}^* = 0$, we can also find that

$$\lambda_{\hat{k}-1}^* - \nu_{\hat{k}-1}^* > 0. \tag{75}$$

Then, using the non-negativity of $\nu_{\hat{k}-1}^*$, we can show that (75) is only possible if $\lambda_{\hat{k}-1}^* > 0$. Thus, using this fact and complementary slackness condition, we conclude that $(\hat{k}-1)$-th constraint in (63) must be active and $(\hat{k}-1)$-th constraint in (65) must be inactive. Thus, the second statement made in property A2 is also proved.

We use contradiction to prove A3. Suppose $\hat{k}$ and $\tilde{k}$ with $\hat{k} < \tilde{k}$ are the indices of two DUs for which both constraints (63) and (65) are inactive. Then, according to property A2, we must have $\lambda_{\hat{k}}^* = \nu_{\hat{k}}^* = \lambda_{\hat{k}}^* - \nu_{\hat{k}}^* = 0$ and $\lambda_{\tilde{k}}^* = \nu_{\tilde{k}}^* = \lambda_{\tilde{k}}^* - \nu_{\tilde{k}}^* = 0$. However, this condition contradicts with (74) and its following extension

$$\lambda_1^* - \nu_1^* > \lambda_2^* - \nu_2^* > \cdots > \lambda_K^* - \nu_K^*. \tag{76}$$

Hence, there can only be one DU for which both constraints (63), (65) are inactive, simultaneously. This proves the property A3 for the case when $\rho^* > 0$. The proof of the theorem is thus complete. ■

B. EXTENSION TO IMPERFECT SIC SCENARIO

In order to model the imperfections of the SIC, we have used SIC imperfection factor $\varkappa$ [56]. With such a modeling of the SIC imperfections, the total noise contribution owing to the imperfect SIC at the k-th DU for decoding the l-th DU signal is given as

$$\varkappa|h_k|^2\sum_{z=1}^{l-1}P_z^{L_z^t}. \tag{77}$$

A more detailed discussion about the SIC imperfection factor can be found in [56], [57], [58] and references therein. Hence, the SINR for decoding the l-th DU's signal at the k-th DU is given as

$$SINR_l^k=\frac{|h_k|^2P_l^{L_l^t}}{|h_k|^2\sum_{j=l+1}^{K}P_j^{L_j^t}+\varkappa|h_k|^2\sum_{z=1}^{l-1}P_z^{L_z^t}+\sigma_k^2}. \tag{78}$$

Then, for fixed values of $\mathscr{L}$, and L_k^t along with the decoding order chosen as suggested in Section IV-A the transmission power minimization problem in the presence of imperfect SIC is given as

$$\begin{aligned}&\min_{P_k^{L_k^t}}\ \sum_{k=1}^{K}P_k^{L_k^t}\\ &\text{s.t}\ \ P_k^{L_k^t}\geq 0,\\ &\min_{i=1,\ldots,k}\ \frac{P_i^{L_i^t}-\left(2^{L_i^t}-1\right)\left(\varkappa\sum_{z=1}^{i-1}P_z^{L_z^t}+\sum_{j=i+1}^{K}P_j^{L_j^t}\right)}{2^{L_i^t}-1}\geq\delta_k.\end{aligned}$$

After some manipulations,[4] it can be shown that the optimal solution of **P-SIC-Imp** must satisfy the following set of linear equations

$$P_k^{L_k^t*}-\left(2^{L_k^t-1}\right)\left(\varkappa\sum_{j=1}^{k-1}P_j^{L_j^t*}+\sum_{i=k+1}^{K}P_i^{L_i^t*}\right)=\left(2^{L_k^t}-1\right)\delta_k. \tag{79}$$

Note that (79) can be written in matrix form as

$$\nabla\mathbf{p}^*=\mathbf{x}, \tag{80}$$

where $\mathbf{p}=[P_1^{L_1^t},\ldots,P_k^{L_K^t}]^T$, $\mathbf{x}=[(2^{L_1^t}-1)\delta_1,\ldots,(2^{L_K^t}-1)\delta_K]^T$. Moreover, (i,i)-th element of ∇ is 1, (i,j)-th element is $-(2^{L_i^t}-1)$, $\forall\, j>i$, and (i,k)-th element is $-\varkappa(2^{L_i^t}-1)$, $\forall\, k<i$. Hence, the closed-form solution for **P-SIC-Imp** is given as

$$\mathbf{p}^*=\nabla^{-1}\mathbf{x}. \tag{81}$$

It is difficult to theoretically analyze the affects of choosing the values of L_k^t. However, in the simulation results section, we illustrate the difference in transmission energy consumption when L_k^t are chosen randomly and according to the PLFs of the DUs as suggested in Section IV-A. In particular, it is shown that choosing L_k^t according to the PLFs of the DUs results in smaller transmission energy consumption and subsequently smaller overall energy consumption.

4. Specifically, noting that $\delta_1>\delta_2>\cdots>\delta_K$ and that the second constraint in **P-SIC-Imp** must be met with equality in optimal solution.

C. SOLVING P2 FOR FIXED VALUE OF $\mathscr{L}$

For a fixed feasible value of $\mathscr{L}=\mathrm{L}$, problem **P2** can be written as follows:

P4:

$$\min_{P_k^{L_k^t},L_k^t,t_k^t}\ \sum_{k=1}^{K}t_k^tP_k^{L_k^t} \tag{82}$$

$$\text{s.t.}\quad 0\leq P_k^{L_k^t}, \tag{83}$$

$$\mathbb{P}_{out}^{k,L_k^t}\leq\theta_k, \tag{84}$$

$$L^{min}\leq L_k^t, \tag{85}$$

$$\sum_{k=1}^{K}L_k-L_k^t\leq\mathrm{L} \tag{86}$$

$$L_k-L_k^t\geq 0, \tag{87}$$

$$0<t_k^t, \tag{88}$$

$$\sum_{k=1}^{K}t_k^t\leq t_t \tag{89}$$

We have following lemma for **P4**.

Lemma 5: The following optimization problem is equivalent to **P4**.

P5:

$$\min_{L_k^t,t_k^t}\ \sum_{k=1}^{K}\delta_kt_k^t\left(2^{\frac{L_k^t}{t_k^t}}-1\right) \tag{90}$$

$$\text{s.t.}\quad \sum_{k=1}^{K}t_k^t\leq t_t, \tag{91}$$

$$0<t_k^t, \tag{92}$$

$$L^{min}\leq L_k^t, \tag{93}$$

$$\sum_{k=1}^{K}L_k-L_k^t\leq\mathrm{L}, \tag{94}$$

$$L_k-L_k^t\geq 0. \tag{95}$$

Proof: For exponentially distributed channel gains with parameter Λ_k, the OP $\mathbb{P}_{out}^{k,L_k^t}$ can be written as

$$\mathbb{P}_{out}^{k,L_k^t}=1-e^{-\frac{\sigma_k^2\Lambda_k}{P_k^{L_k^t}}\left(2^{\frac{L_k^t}{t_k^t}}-1\right)}. \tag{96}$$

Hence, the constraint on the OP can be equivalently written as

$$\frac{\sigma_k^2\Lambda_k}{\ln\left(\frac{1}{1-\theta_k}\right)}\left(2^{\frac{L_k^t}{t_k^t}}-1\right)\leq P_k^{L_k^t}. \tag{97}$$

Since, the objective function of **P4** is increasing with $P_k^{L_k^t}$, we must chose the smallest feasible value of $P_k^{L_k^t}$. Then, after putting

$$P_k^{L_k^t} = \frac{\sigma_k^2 \Lambda_k}{\ln\left(\frac{1}{1-\theta_k}\right)}\left(2^{\frac{L_k^t}{t_k}} - 1\right), \tag{98}$$

we obtain (90). The proof is completed. ■

It is straightforward to show that **P5** is a convex optimization problem. Hence, we can use off-the-shelf optimization tools, such as CVX, to solve **P5**. However, in the following we use KKT conditions to solve **P5** to gain insight into the optimal solution, which can reduce the complexity of the algorithm for solving the optimization problem.

We have following theorem about the optimal solution for **P5**.

Theorem 2: The optimal solution of **P5** has following properties.

- A4: Constraint (91) is always active.
- A5: If $\mathscr{A}$ denote the set of DUs for which both constraints (93) and (95) are inactive simultaneously, then $|\mathscr{A}| \leq 1$, where $|\mathscr{A}|$ denotes the cardinality of $\mathscr{A}$.
- A6: If for $\hat{k}$-th DU both the constraints (93) and (95) are inactive, then for $(\hat{k}+1)$-th DU, the constraint (93) is inactive and constraint (95) is active. Furthermore, for $(\hat{k}-1)$-th DU the constraint (93) must be active and the constraint (95) must be inactive.

Proof: The partial Lagrangian[5] for **P5** can be written as follows.

$$\begin{aligned}\mathcal{L}(\alpha,\gamma,\phi,\Upsilon,L_k^t) &= \sum_{k=1}^{K}\delta_k t_k^t\left(2^{\frac{L_k^t}{t_k^t}} - 1\right) + \alpha\Big(\sum_{k=1}^{K} t_k^t - t_t\Big) \\ &+ \sum_{k=1}^{K}\gamma_k(L_k^{min} - L_k^{t*}) + \phi\Big(\sum_{k=1}^{K} L_k - L_k^t - \mathrm{L}\Big) \\ &+ \sum_{k=1}^{K}\Upsilon_k\big(L_k^t - L_k\big),\end{aligned} \tag{99}$$

where $\alpha \geq 0, \gamma_k \geq 0, \phi \geq 0, \Upsilon_k$ are dual variables for constraints (91), (93), (94) and (95), respectively. Then, the corresponding KKT conditions can be formulated as

$$\alpha^*\left(\sum_{k=1}^{K} t_k^{t*} - t_t\right) = 0, \tag{100}$$

$$\gamma_k^*(L^{min} - L_k^{t*}) = 0, \ \ \forall k \in \{1,2,\ldots,K\}, \tag{101}$$

$$\phi^*\left(\sum_{k=1}^{K} L_k - L_k^{t*} - \mathrm{L}\right) = 0, \tag{102}$$

$$\Upsilon_k^*\big(L_k^{t*} - L_k\big) = 0, \ \ \forall k \in \{1,2,\ldots,K\}, \tag{103}$$

$$\delta_k\left(2^{\frac{L_k^{t*}}{t_k^{t*}}} - \frac{L_k^{t*}\ln(2)2^{\frac{L_k^{t*}}{t_k^{t*}}}}{t_k^{t*}} - 1\right) + \alpha^* = 0, \ \ \forall k \in \{1,2,\ldots,K\}, \tag{104}$$

$$-\delta_k \ln(2) 2^{\frac{L_k^{t*}}{t_k^{t*}}} + \gamma_k^* - \Upsilon_k^* + \phi^* = 0, \ \ \forall k \in \{1,2,\ldots,K\}, \tag{105}$$

$$\alpha^* \geq 0, \gamma_k^* \geq 0, \phi^* \geq 0, \Upsilon_k^* \geq 0. \tag{106}$$

Note that $f(x) = 2^x(1 - x\ln(2))$ is a decreasing function of x with $\lim_{x\to 0} f(x) = 1$. Hence, it can be easily deduced from (104) that $\alpha^* > 0$ since $2^{\frac{L_k^{t*}}{t_k^{t*}}}(1 - \frac{L_k^{t*}}{t_k^{t*}}\ln(2)) < 1$ for all finite $t_k^{t*} \geq 0$. Therefore, according to complementary slackness condition in (100), we must have

$$\sum_{k=1}^{K} t_k^{t*} - t_t = 0. \tag{107}$$

Thus, property A4 is proved.

Next, we prove property A5 with the help of contradiction. For any two distinct DUs, $i, j \in \{1,2,\ldots,K\}$, we can obtain following relations from (104)

$$\alpha^* = \delta_i\left(1 - 2^{\frac{L_i^{t*}}{t_i^{t*}}}\left(1 - \frac{L_i^{t*}}{t_i^{t*}}\ln(2)\right)\right), \tag{108}$$

$$\alpha^* = \delta_j\left(1 - 2^{\frac{L_j^{t*}}{t_j^{t*}}}\left(1 - \frac{L_j^{t*}}{t_j^{t*}}\ln(2)\right)\right). \tag{109}$$

From (108), (109) and using the fact that $f(x)$ is a decreasing function, we can show that if $\delta_i > \delta_j$ then $\frac{L_j^{t*}}{t_j^{t*}} > \frac{L_i^{t*}}{t_i^{t*}}$. By equating (108), (109), we get

$$\frac{\delta_i}{\delta_j} = \frac{1 - 2^{\frac{L_j^{t*}}{t_j^{t*}}}\left(1 - \frac{L_j^{t*}}{t_j^{t*}}\ln(2)\right)}{1 - 2^{\frac{L_i^{t*}}{t_i^{t*}}}\left(1 - \frac{L_i^{t*}}{t_i^{t*}}\ln(2)\right)}. \tag{110}$$

On the other hand, (105) can be rearranged in the following form for DUs i and j

$$\phi = \delta_i \ln(2) 2^{\frac{L_i^{t*}}{t_i^{t*}}} - \gamma_i^* + \Upsilon_i^*, \tag{111}$$

$$\phi = \delta_j \ln(2) 2^{\frac{L_j^{t*}}{t_j^{t*}}} - \gamma_j^* + \Upsilon_j^*. \tag{112}$$

From (111), (112), we get

$$\delta_i 2^{\frac{L_i^{t*}}{t_i^{t*}}} - \delta_j 2^{\frac{L_j^{t*}}{t_j^{t*}}} = \frac{\left(\gamma_i^* - \Upsilon_i^*\right) - \left(\gamma_j^* - \Upsilon_j^*\right)}{\ln(2)}. \tag{113}$$

5. Note that we have ignored the terms due to the constraints $t_k \geq 0$ since these constraints are always inactive and hence the corresponding dual variables will be zero.

If we assume that $\gamma_i^* - \Upsilon_i^* = \gamma_j^* - \Upsilon_j^*$, then according to (110) and (113) we must have

$$\frac{1 - 2^{\frac{L_j^{t*}}{t_j^{t*}}}\left(1 - \frac{L_j^{t*}}{t_j^{t*}}\ln(2)\right)}{1 - 2^{\frac{L_i^{t*}}{t_i^{t*}}}\left(1 - \frac{L_i^{t*}}{t_i^{t*}}\ln(2)\right)} = \frac{2^{\frac{L_j^{t*}}{t_j^{t*}}}}{2^{\frac{L_i^{t*}}{t_i^{t*}}}}. \tag{114}$$

We can rearrange (114) as follows:

$$2^{-\frac{L_j^{t*}}{t_j^{t*}}} + \frac{L_j^{t*}}{t_j^{t*}}\ln(2) = 2^{-\frac{L_i^{t*}}{t_i^{t*}}} + \frac{L_i^{t*}}{t_i^{t*}}\ln(2). \tag{115}$$

However, (115) cannot be true because $g(x) = 2^{-x} + x\ln(2)$ is an increasing function of x. Therefore, we conclude that $\gamma_i^* - \Upsilon_i^*$ and $\gamma_j^* - \Upsilon_j^*$ have distinct values. That is

$$\gamma_i^* - \Upsilon_i^* \neq \gamma_j^* - \Upsilon_j^*, \quad i, j \in \{1, \ldots, K\}, i \neq j. \tag{116}$$

This means that at most one $\gamma_k^* - \Upsilon_k^*$ can be zero. Also, using the fact that $\gamma_k^*, \Upsilon_k^* \geq 0, \forall k \in \{1, 2, \ldots, K\}$ and the complementary slackness conditions (101), (103), we conclude that there can be only one DU for which both constraints (93), (95) can be inactive simultaneously. This proves property A5.

Next, we prove A6. Note that we can arrange (113) as

$$\frac{\delta_i}{\delta_j} 2^{\frac{L_i^{t*}}{t_i^{t*}}} - 2^{\frac{L_j^{t*}}{t_j^{t*}}} = \frac{\left(\gamma_i^* - \Upsilon_i^*\right) - \left(\gamma_j^* - \Upsilon_j^*\right)}{\delta_j \ln(2)}. \tag{117}$$

Using (110), we can arrange the left hand side of (117) as

$$\frac{\delta_i}{\delta_j} 2^{\frac{L_i^{t*}}{t_i^{t*}}} - 2^{\frac{L_j^{t*}}{t_j^{t*}}} = \frac{2^{-\frac{L_j^{t*}}{t_j^{t*}}} + \frac{L_j^{t*}}{t_j^{t*}}\ln(2) - 2^{-\frac{L_i^{t*}}{t_i^{t*}}} - \frac{L_i^{t*}}{t_i^{t*}}\ln(2)}{1 - 2^{\frac{L_i^{t*}}{t_i^{t*}}}\left(1 - \frac{L_i^{t*}}{t_i^{t*}}\ln(2)\right)}. \tag{118}$$

Also, we note that if $\delta_i > \delta_j$, then we must have $\frac{L_j^{t*}}{t_j^{t*}} > \frac{L_i^{t*}}{t_i^{t*}}$ according to (108) and (109). Using this fact, the monotonic increasing property of $g(x)$, and the fact that $1 - 2^{\frac{L_i^{t*}}{t_i^{t*}}}(1 - \frac{L_i^{t*}}{t_i^{t*}}\ln(2)) > 0$, we can conclude that

$$\frac{\delta_i}{\delta_j} 2^{\frac{L_i^{t*}}{t_i^{t*}}} - 2^{\frac{L_j^{t*}}{t_j^{t*}}} > 0 \tag{119}$$

whenever $\delta_i > \delta_j$. Therefore, we must have

$$\left(\gamma_i^* - \Upsilon_i^*\right) - \left(\gamma_j^* - \Upsilon_j^*\right) > 0, \text{ if } \delta_i > \delta_j. \tag{120}$$

Then, assuming, without loss of generality, that the DUs are ordered in such a way that their PLFs can be ordered as $\delta_1 > \delta_2 > \cdots > \delta_k$, the optimality condition (120) can be extended to the following generalized condition

$$\gamma_1^* - \Upsilon_1^* > \gamma_2^* - \Upsilon_2^* > \cdots > \gamma_K^* - \Upsilon_K^*. \tag{121}$$

Assume that for $\hat{k}$-th DU both constraints (93) and (95) are inactive. Then, due to complementary slackness conditions both $\gamma_{\hat{k}}^*$ and $\Upsilon_{\hat{k}}^*$ must be zero. Therefore, (121) can be true only if $\gamma_{\hat{k}+1}^* < \Upsilon_{\hat{k}+1}^*$. However, if $\Upsilon_{\hat{k}+1}^*$ is positive, then constraint (95) for $(\hat{k}+1)$-th DU must be active. This also leads to the conclusion that $(\hat{k}+1)$-th constraint in (93) is inactive. This proves the first part stated in property A6.

Now we consider the second statement made in property A6. From (121) and the fact that $\gamma_{\hat{k}}^* = \Upsilon_{\hat{k}}^* = 0$, we can also find that

$$\gamma_{\hat{k}-1}^* - \Upsilon_{\hat{k}-1}^* > 0. \tag{122}$$

Then, using the non-negativity of $\Upsilon_{\hat{k}-1}^*$, we can show that (122) is only possible if $\gamma_{\hat{k}-1}^* > 0$. Thus, using this fact and complementary slackness condition (101), we conclude that $(\hat{k}-1)$-th constraint in (93) must be active and $(\hat{k}-1)$-th constraint in (95) must be inactive. Therefore, the second statement made in property A6 is also proved. ■

With the help of Theorem 2, the problem **P5** can be simplified to the following problem

$$\mathbf{P6}: \min_{t_k^t} \sum_{k=1}^{K} \delta_k t_k^t \left(2^{\frac{r_k}{t_k^t}} - 1\right) \tag{123}$$

$$\text{s.t.} \sum_{k=1}^{K} t_k^t \leq t_t, \tag{124}$$

where $r_k = L^{min}$ for $k \in \{1, 2, \ldots, \hat{k}-1\}$, $r_{\hat{k}} = L_{\hat{k}} - (L - \sum_{k=1}^{\hat{k}-1}(L_k - L^{min}))$, and $r_k = L_k \ \forall k \in \{\hat{k}+1, \ldots, K\}$. We have following lemma for problem **P6**.

Lemma 6: The optimal solution of t_k^t can be found from solving following relation

$$t_k^t = \frac{r_k \ln(2)}{\mathcal{W}\left(\frac{\alpha - \delta_k}{e\delta_k}\right) + 1}, \tag{125}$$

where α is the dual variable associated with constraint of problem **P6** and α^* satisfies following relation

$$\sum_{k=1}^{K} \frac{r_k \ln(2)}{\mathcal{W}\left(\frac{\alpha - \delta_k}{e\delta_k}\right) + 1} = t^t, \tag{126}$$

where $\mathcal{W}(.)$ is the Lambert W function.

Proof: We can write the Lagrangian of problem **P6** as

$$\mathcal{L}(\alpha) = \sum_{k=1}^{K} \delta_k t_k^t \left(2^{\frac{r_k}{t_k^t}} - 1\right) + \alpha\left(\sum_{k=1}^{K} t_k^t - t_t\right). \tag{127}$$

After taking the derivative of (127) with respect to t_k^t and equating it to zero, we get

$$\alpha^* = \delta_k\left(1 - 2^{\frac{r_k}{t_k^t}}\left(1 - \frac{r_k}{t_k^t}\ln(2)\right)\right). \tag{128}$$

We can rewrite (128) as

$$2^{\frac{r_k}{t_k^t}}\left(1 - \frac{r_k}{t_k^t}\ln(2)\right) = \frac{\delta_k - \alpha^*}{\delta_k}. \tag{129}$$

Let us introduce a new variables $z_k = \frac{r_k}{t_k^t}$ for simplification. Then, we can write (129) as

$$\frac{\delta_k - \alpha^*}{\delta_k} = e^{z_k \ln(2)}(1 - z_k \ln(2)). \tag{130}$$

Multiplying both side of (130) with e^{-1} we get

$$\frac{\alpha^* - \delta_k}{\delta_k} e^{-1} = e^{z_k \ln(2) - 1}(z_k \ln(2) - 1). \tag{131}$$

The right hand side of (131) is of the form xe^x. Therefore, we can apply the Lambert $\mathcal{W}$ function on both sides of (131) to get

$$z_k \ln(2) - 1 = \frac{r_k}{t_k^t} \ln(2) - 1 = \mathcal{W}\left(\frac{\alpha^* - \delta_k}{\delta_k e}\right). \tag{132}$$

From which we can obtain the following relation

$$t_k^t = \frac{r_k \ln(2)}{1 + \mathcal{W}\left(\frac{\alpha^* - \delta_k}{\delta_k e}\right)}. \tag{133}$$

This proves (125).

Since $1 - f(x)$ is an increasing function of x, and since $t_k^{t*} \neq 0$ we always have $\alpha^* > 0$. This means the constraint (124) must be active. Once the value of α^* is found, the value of t_k^{t*} can be obtained from (125). Next, we prove (126). As mentioned before, the constraint (124) must be active. Then, according to the strict equality of (124) and the equality (125) we must have

$$\sum_{k=1}^{K} \frac{r_k \ln(2)}{\mathcal{W}\left(\frac{\alpha - \delta_k}{e\delta_k}\right) + 1} = t^t. \tag{134}$$

The proof is complete. ■

The Lambert $\mathcal{W}(.)$ function requires higher computational complexity. Specifically, the computational operations needed for computing $\mathcal{W}(.)$ by iterative Hallye's method with p iterations are $6p$ additions, $5p$ multiplications and $2p$ exponentiations [59]. Therefore, it is not computationally efficient to find the optimal value of α^* through Bisection search from (126). To this end, a low complexity iterative algorithm (LCIA) is provided in the following for finding the optimal value of α^*.

Before providing the details of LCIA, we define the following variables for notational convenience:

$$\alpha_k = \delta_k \left(1 - 2^{\frac{r_k}{t_k^t}} \left(1 - \frac{r_k}{t_k^t} \ln(2)\right)\right) > 0. \tag{135}$$

The LCIA has two main steps. The first step deals with the individual time allocations, while the second step involves updating of α. More precisely, the two steps can be described as follows:

- Step 1: For a given value of α, find t_k^t using (125) and normalize t_k^t so that $\tau_k^t = \frac{t^t t_k^t}{\sum_{k=1}^K t_k^t}$, and $\sum_{k=1}^K \tau_k^t = t^t$.
- Step 2: For given normalized values of t_k^t (that is τ_k^t), find α_k using (135). Then, before introducing the update rule for α, we provide the following lemma which highlight useful properties of α^* and α_k that can be used to obtain the update rule for α.

Lemma 7: For given $\alpha_k(t_k^t)$ and $t_k^t(\alpha)$, in the i-th iteration of the LCIA, we have following relationship among $\alpha^{(i-1)}, \alpha_k^{(i)}, \alpha^*$:

- If $\alpha^{(i-1)} > \alpha^*$ then

$$\alpha^* < \max_k\{\alpha_k^{(i)}\} < \alpha^{(i-1)}, \tag{136}$$

and

$$\sum_{k=1}^{K} \tau_k^{t^{(i)}} < t^t. \tag{137}$$

- If $\alpha^{(i-1)} < \alpha^*$, then

$$\alpha^{(i-1)} < \min_k\left\{\alpha_k^{(i)}\right\} < \alpha^*, \tag{138}$$

and

$$\sum_{k=1}^{K} \tau_k^{t^{(i)}} > t^t. \tag{139}$$

where $\alpha_k^{(i)} = \alpha_k(\tau_k^{t^{(i)}})$ and $\tau_k^{t^{(i)}} = \frac{t^t t_k^{t^{(i)}}}{\sum_{k=1}^K t_k^{t^{(i)}}}$.

Proof: First, note the following properties

- A7: According to (125), t_k^t is a decreasing function of α.
- A8: According to (135), α_k is a decreasing function of t_k^t.

If $\alpha^{(i-1)} > \alpha^*$, then according to property A7 we have $t_k^t(\alpha^{(i-1)}) < t_k^t(\alpha^*)$. Hence, $\sum_{k=1}^K t_k^{t^{(i)}} < \sum_{k=1}^K t_k^t(\alpha^*) = t^t$ and $\tau_k^{t^{(i)}} = \frac{t^t t_k^{t^{(i)}}}{\sum_{k=1}^K t_k^{t^{(i)}}} > t_k^{t^{(i)}}$. Now, from the decreasing property of α_k we have $\alpha_k(\tau_k^{t^{(i)}}) < \alpha_k(t_k^{t^{(i)}}) \leq \max_k\{\alpha_k^{i-1}\} = \alpha^{(i-1)}$. Therefore, we have $\max_k\{\alpha_k^{(i)}\} < \alpha^{(i-1)}$. This proves the right hand inequality of (136). Now we prove the left hand inequality of (136). Assume that $\max_k\{\alpha_k(\tau_k^{t^{(i)}})\} < \alpha^*$ and therefore $\alpha_k(\tau_k^{t^{(i)}}) < \alpha^*$, $\forall k \in \{1, 2, \ldots, K\}$. Then, according to property A7, we have $t_k^t(\alpha^*) < \tau_k^{t^{(i)}}$ which results in $t^t = \sum_{k=1}^K t_k^t(\alpha^*) < \sum_{k=1}^K \tau_k^{t^{(i)}}$. However, this is contradictory to the definition of τ_k^t. Therefore, we conclude that $\max_k\{\alpha_k(\tau_k^{t^{(i)}})\} < \alpha^*$ cannot be true if $\alpha^{(i-1)} > \alpha^*$. Hence, (136) and (137) are proved.

A similar line of reasoning can be used to prove (138) and (139). ■

Based on Lemma 7, the updated value of α in the i-th iteration can be written as follows

$$\alpha^{(i)} = \begin{cases} \max_k\{\alpha_k^{(i)}\}, & \text{if } \sum_{k=1}^K t_k^t > t_t, \\ \min_k\{\alpha_k^{(i)}\}, & \text{if } \sum_{k=1}^K t_k^t < t_t. \end{cases} \tag{140}$$

The overall LCIA algorithm for solving **P6** is depicted in **Algorithm 1**.

Algorithm 1: LCIA: Algorithm for Finding Optimal Value of α^* in **P6** for Given Initial Values of α_k and Tolerance $\epsilon \to 0$

while $|z - t^t| > \epsilon$ **do**
  Calculate t_k^t according to (135) for given α_k;
  Calculate $z = \sum_{k=1}^{K} t_k^t$;
  Calculate $\tau_k^t \ \forall k \in \{1, 2, \ldots, K\}$;
  Calculate α_k according to (135) for given τ_k^t;
  Set α according to (140);
end

Algorithm 2: Proposed Algorithm for **P1** in a Single-Cell Scenario

1 Set E_{min} to be a very high value, and υ to be a very small value;
2 Sort PLFs such that $\delta_1 > \delta_2 > \cdots > \delta_K$;
3 **for** $\mathscr{L} = 0 : \upsilon : \sum_{k=1}^{K} L_k - L_k^{min}$ **do**
4 Set $k = 1$;
5 Set $\hat{\mathscr{L}} = \mathscr{L}$;
6 **while** $\hat{\mathscr{L}} > \left(L_k - L_k^{min}\right)$ **do**
7 $L_k^t = L_k^{min}$;
8 $\hat{\mathscr{L}} = \mathscr{L} - \left(L_k - L_k^{min}\right)$;
9 Set $k = k + 1$;
10 **end**
11 **if** $\hat{\mathscr{L}} > 0$ **then**
12 Set $L_k^t = L_k - \hat{\mathscr{L}}$;
13 **end**
14 Find the individual users transmit powers $P_k^{L_k^t}$ for obtained L_k^t from (57);
15 Find the compression energy, $E_c^{\mathscr{L}}$, from (4);
16 Compute the total energy consumption as $E_T^{\mathscr{L}} = E_c^{\mathscr{L}} + t^t \sum_{k=1}^{K} P_k^{L_k^t}$;
17 **if** $E_{min} > E_T^{\mathscr{L}}$ **then**
18 $E_{min} = E_T^{\mathscr{L}}$;
19 $L_k^{t*} = L_k^t, \mathscr{L}^* = \mathscr{L}$;
20 **end**
21 **end**

Algorithm 3: Proposed Algorithm for **P2** in a Single-Cell Scenario

1 Set E_{min} to be a very high value, and υ to be a very small value;
2 Sort PLFs such that $\delta_1 > \delta_2 > \cdots > \delta_K$;
3 **for** $\mathscr{L} = 0{:}\upsilon{:} \sum_{k=1}^{K} L_k - L_k^{min}$ **do**
4 Set $k = 1$;
5 Set $\hat{\mathscr{L}} = \mathscr{L}$;
6 **while** $\hat{\mathscr{L}} > \left(L_k - L_k^{min}\right)$ **do**
7 $L_k^t = L_k^{min}$;
8 $\hat{\mathscr{L}} = \mathscr{L} - \left(L_k - L_k^{min}\right)$;
9 Set $k = k + 1$;
10 **end**
11 **if** $\hat{\mathscr{L}} > 0$ **then**
12 Set $L_k^t = L_k - \hat{\mathscr{L}}$;
13 **end**
14 Use Algorithm 1 to find the values of t_k^t;
15 Find the individual users transmit powers for obtained L_k^t and t_k^t from (98);
16 Find the compression energy, $E_c^{\mathscr{L}}$, from (4);
17 Compute the total energy consumption as $E_T^{\mathscr{L}} = E_c^{\mathscr{L}} + t^t \sum_{k=1}^{K} P_k^{L_k^t}$;
18 **if** $E_{min} > E_T^{\mathscr{L}}$ **then**
19 $E_{min} = E_T^{\mathscr{L}}$;
20 $L_k^{t*} = L_k^t, \mathscr{L}^* = \mathscr{L}$;
21 **end**
22 **end**

D. PROPOSED ALGORITHMS FOR PROBLEMS P1 AND P2

Based on the analysis presented in Sections IV-A and IV-C, we present efficient optimization algorithms for solving **P1** and **P2**. The proposed algorithm for solving **P1** is provided as **Algorithm 2** and the proposed algorithm for solving **P2** is provided as **Algorithm 3**.

The 2nd line of both algorithms sort the values of PLFs. Then, for a given value of $\mathscr{L}$, both algorithms find the optimal transmission rate for individual DUs through lines $4-13$. Subsequently, lines $14-16$, and $14-17$ find the optimal transmission power and compression energy in **Algorithm 2** and **Algorithm 3**, respectively. Then, the check for optimality and saving of optimal solution is done in lines $17-20$, and $18-21$ in **Algorithm 2** and **Algorithm 3**, respectively.

V. PROPOSED SOLUTION FOR OVERALL ENERGY CONSUMPTION MINIMIZATION IN MULTI-CELL SCENARIO

In order to extend the system model to multi-cell scenario, we assume there are M BSs and the m-th BS serves $K(m)$ number of DUs. Note that while the recent works [23], [33] have considered multi-cell scenarios with NOMA transmission, their system model assumed that at most two DUs are associated with one BS on a single frequency band. Moreover, the proposed algorithms in [23], [33] require estimates of instantaneous CSI for solving the formulated optimization problems. In the following, it is assumed that the BS-DU association is given. Moreover, Table 2 provides the important notations used in this section. Next, Section V-A and V-B describe the proposed approach for minimizing the overall energy consumption in a multi-cell scenario with NOMA and OMA transmissions, respectively.

A. MULTI-CELL PROBLEM WITH NOMA TRANSMISSIONS

Note that for single-cell scenario the global optimal solution is achievable and provable with the help of convex

TABLE 2. Summary of notations used for multi-cell scenario.

Parameter	Value
number of BSs	M
number of DUs associated with m-th BS	$K(m)$
k-th DU of the m-th BS	$k(m)$
distance between $k(m)$-th DU and m-th BS	d_k
distance between $k(m)$-th DU to $r \neq m$-th BS	$\hat{d}_k^r$
channel between $k(m)$ and r-th BS	$h_{k,m,r}$
order of decoding for m-th BS	χ_m
transmit power dedicated for $k(m)$ DU	$P_{k,m}$
transmit power dedicated for $k(m)$ DU in Q-th iteration	$P_{k,m}^Q$
total transmit power of m-th BS	$\hat{P}_m$
adjusted noise power for $k(m)$-th DU	$\hat{\sigma}_{k,m}^2$
total transmission energy	E_t
total compression energy	E_c
compression bits for the m-th BS	$\mathcal{L}_{m,c}$
total transmission energy in b-th iteration	E_t^b
total compression energy in b-th iteration	E_c^b
compression bits for the m-th BS in b-th iteration	$\mathcal{L}_{m,c}^b$

optimization theory and KKT conditions. However, it is not possible to make such claims for multi-cell scenario. Therefore, in the following an iterative scheme is devised where the objective function is guaranteed to be non-increasing in successive iterations. This is an important property for the iterative algorithms since otherwise it is not possible to prove the convergence of the overall algorithm.

In order to develop an iterative algorithm for multi-cell scenario, we use the observations obtained through the analysis of single cell scenario. Precisely, we use the following two observations about the optimal power allocation in the single cell scenario.

- The optimal value of the total transmit power is increasing with the PLF of the DUs.
- The value of PLF for the k-th DU is directly proportional to the noise power σ_k^2.

These observations can be easily verified by looking at the mathematical expressions of optimal value of the transmit power for NOMA in (57) and the definition of PLF.

The proposed algorithm for the multi-cell scenario is provided as **Algorithm 4**. Specifically, in step 3 the total compression energy is calculated for a fixed value of $\{\mathcal{L}_{m,c}\}$. Then, in step 4 **Algorithm 4** uses **Algorithm 5** to find the optimal values of transmission powers for individual BSs in an iterative manner. The working principle of **Algorithm 5** relies on solving the optimization problem similar to those studied in Section IV-A for the single cell scenario, except that the interference caused by the signals transmitted by the other BSs is also treated as noise. Hence, the adjusted noise power for the $k(m)$-th DU is given as

$$\hat{\sigma}_{k,m}^2 = \sigma_{k,m}^2 + \sum_{r=1,r\neq m}^{M} h_{k,m,r} \sum_{k=1}^{K(r)} P_{k,r}^*,$$

Algorithm 4: Proposed Algorithm for NOMA Multi-Cell Problem

1 **Initialize**: Set E^{min} to a very high value and obtain the set of all possible combinations of compressed bits for individual BSs as $\mathcal{C} = \{\mathcal{L}_1^c, \ldots, \mathcal{L}_{|\mathcal{C}|}^c\}$, where $\mathcal{L}_b^c = \{\mathcal{L}_{1,c}^b, \ldots, \mathcal{L}_{M,c}^b\}$;
2 **for** $b = 1 : |\mathcal{C}|$ **do**
3 **Calculate:** $E_c^b = \sum_{m=1}^{M} E_{m,c}^b$ by using $\mathcal{L}_{m,c} = \mathcal{L}_{m,c}^b$ for finding $E_{m,c}^b$;
4 Obtain the optimal total transmission energy by applying **Algorithm 5** and save it as E_t^b;
5 **if** $E_t^b + E_c^b \leq E^{min}$ **then**
6 $E^{min} = E_t^b + E_c^b$;
7 Set $\mathcal{L}_{m,c}^* = \mathcal{L}_{m,c}^b$;
8 **end**
9 **end**

Algorithm 5: Proposed Algorithm for NOMA Multi-Cell Problem With Fixed Values of Compressed Bits for Each BS

1 **Initialize**: Start from feasible values of $\hat{P}_1^0 = \hat{P}_1, \ldots, \hat{P}_M^0 = \hat{P}_M$;
2 **Calculate**: PLFs for all the users within the system by using the noise power given by (138);
3 **for** $Q = 1 : \hat{M}$ **do**
4 **if** $Q \ mod \ M = 0$ **then**
5 $m = M$;
6 **end**
7 **else**
8 $m = Q \ mod \ M$;
9 **end**
10 Obtain the global optimal total transmit power for m-th BS, denoted by P_m^*, for given values of PLFs of its associated DUs as suggested in Section IV-A;
11 Set $P_{\hat{m}}^{Q*} = P_{\hat{m}}^{Q-1}$, $\forall\ \hat{m} \in \{1, \ldots, M\} \setminus m$ and $P_m^{Q*} = P_m^*$;
12 Update the PLFs of all the users associated with the remaining BSs;
13 **end**
14 **Output:** Set $E_t = \sum_{m=1}^{M} P_m^{Q*}$.

$$= \sigma_{k,m}^2 + \sum_{r=1,r\neq m}^{M} h_{k,m,r} \hat{P}_r^*. \tag{141}$$

Next, the detailed description of **Algorithm 5** and the corresponding initialization step is given as follows.

With a fixed compression energy consumption, in each inner iteration (steps 3-13) **Algorithm 5** minimizes the transmit power consumption at one of the BSs by using power allocation scheme suggested in Section IV-A while keeping the transmit power consumption of the rest of BSs unchanged. Next, in order to illustrate the non-increasing

nature of the total power consumption consider, without loss of generality, the iteration when the transmission power for m-th BS is minimized. Due to the global optimality of $\sum_{k=1}^{K(m)} P_{k,m}^{\mathcal{Q},*}$, we have

$$\hat{P}_m^{\mathcal{Q}*} \triangleq \sum_{k=1}^{K(m)} P_{k,m}^{\mathcal{Q}*} \leq \sum_{k=1}^{K(m)} P_{k,m}^{(\mathcal{Q}-1)*} \triangleq \hat{P}_m^{(\mathcal{Q}-1)*}. \quad (142)$$

Thus, the noise power contributed by the m-th BS to all the DUs associated with $\{1,\ldots,m-1,m+1,\ldots,M\}$ BSs will also be non-increasing in each successive inner iteration. This means that the optimal transmit power obtained in previous iterations at all the $\{1,\ldots,m-1\}$ BSs still satisfy the rate and outage probability constraints of their respective DUs. Moreover, the non-increasing property of the transmit power for m-th BS also means that non-increasing total transmit powers at $\{m+1,\ldots,M\}$ BSs can be obtained in subsequent iterations since each of PLFs associated with all the DUs associated with $\{m+1,\ldots,M\}$ BSs are non-increasing.

Note that **Algorithm 5** requires feasible points of $\hat{P}_m$ initially for its proper operation. To solve this issue, we note that for any given values of total number of compression bits at all the BSs, the total transmit power minimization problem for all the BSs can be formulated as

$$\begin{aligned}\textbf{P7:}\ \min_{P_{k,m},L_{k,m}^t}\ & \sum_{m=1}^{M}\sum_{k=1}^{K(m)} P_{k,m}\\ \text{s.t}\ & 0 \leq P_{k,m},\\ & \Gamma_{k,m}^{L_{k,m}^t} \sum_{j=k+1}^{K(m)} P_{j,m}^{L_{j,m}^t} < P_{k,m}^{L_{k,m}^t},\\ & (143),\\ & L^{min} \leq L_{k,m}^t,\\ & L_{k,m}^t \leq L^{max},\\ & \sum_{k=1}^{K(m)} L^{max} - L_{k,m}^t \leq \mathcal{L}_{m,c}.\end{aligned}$$

Assume that the set $\{\hat{L}_{k(m)}^t\}$ satisfies the last three linear constraints of **P7**, then we can obtain feasible values of $P_{k(m)}$ for **P7** by solving the following optimization problem

$$\begin{aligned}\textbf{P8:}\ \min_{P_{k(m)}}\ & \sum_{m=1}^{M}\sum_{k=1}^{K(m)} P_{k,m}\\ & 0 \leq P_{k,m},\\ & \Gamma_{k,m}^{\hat{L}_{k,m}^t} \sum_{j=k+1}^{K(m)} P_{j,m}^{\hat{L}_{j,m}^t} < P_{k,m}^{\hat{L}_{k,m}^t},\\ & (144).\end{aligned}$$

In **P8**, the objective function and the first two constraints are linear. Moreover, left hand side of (144) as shown at tghe bottom of the page is a point-wise minimum of linear functions, which is a concave function [55], and the right hand side of (144) is a linear function. Therefore, **P8** is a convex optimization problem and we can use standard convex optimization problems solvers, such as CVX, to optimally solve it. After solving **P8**, we can get the feasible values for $\{\hat{P}_m\}$ through the relation $\hat{P}_m \triangleq \sum_{k=1}^{K(m)} P_{k,m}, \forall\ m \in \{1,\ldots,M\}$.

The computational complexity largely depends on solving the feasibility problem **P8** since the inner iterations in **Algorithm 5** use closed-form solutions therefore their complexity is negligible. For the feasibility problem, assuming interior point method, the computational complexity becomes $\mathcal{O}((MK)^{3.5})$ as there are in total MK number of optimization variables.

B. MULTI-CELL PROBLEM WITH OMA TRANSMISSIONS

For OMA transmissions in the multi-cell scenario, we can not adopt the strategy used for NOMA transmissions since the interference power from other cells can not be modeled in the same manner as in NOMA transmissions. This problem arises due to the time scheduled transmissions for individual DUs. This hinders the quantification of the interference terms in the neighboring cell DUs in a multi-cell scenario. To tackle this issue, we model the interference power caused by a cell to be represented by the maximum transmit power allocated among all its associated DUs. Mathematically, the interference experienced by the $k(m)$-th DU is modeled as

$$\tilde{\sigma}_{k,m}^2 = \sigma_{k,m}^2 + \sum_{r=1,r\neq m}^{M} h_{k,m,r} \max_{k\in\{1,\ldots,K(r)\}} P_{k,r}^*. \quad (146)$$

$$\min_{i\in\{1,\ldots,k\}} \frac{P_{i,m}^{L_{i,m}^t} - \left(2^{L_{i,m}^t}-1\right)\sum_{j=i+1}^{K(m)} P_{j,m}^{L_{j,m}^t}}{\left(2^{L_{i,m}^t}-1\right)} \geq \frac{\Lambda_{k,m}\left(\sigma_{k,m}^2 + \sum_{r=1,r\neq m}^{M} h_{k,m,r}\sum_{k=1}^{K(r)} P_{k,r}\right)}{\log\left(\frac{1}{1-\theta_{k,m}}\right)}, \quad (143)$$

$$\min_{i\in\{1,\ldots,k\}} \frac{P_{i,m}^{\hat{L}_{i,m}^t} - \left(2^{\hat{L}_{i,m}^t}-1\right)\sum_{j=i+1}^{K(m)} P_{j,m}^{\hat{L}_{j,m}^t}}{\left(2^{\hat{L}_{i,m}^t}-1\right)} \geq \frac{\Lambda_{k,m}\left(\sigma_{k,m}^2 + \sum_{r=1,r\neq m}^{M} h_{k,m,r}\sum_{k=1}^{K(r)} P_{k,r}\right)}{\log\left(\frac{1}{1-\theta_{k,m}}\right)}, \quad (144)$$

$$\bar{\mathbf{P}}_{k,m} = \left[P_{1,1}^{L_{1,1}^{t*}},\ldots,P_{K,1}^{L_{K,1}^{t*}},\ldots,P_{k-1,m}^{L_{k-1,m}^{t*}},P_{k+1,m}^{L_{k+1,m}^{t*}},\ldots,P_{1,M}^{L_{1,M}^{t*}},\ldots,P_{K,M}^{L_{K,M}^{t*}}\right], \quad (145)$$

Hence, the transmission energy minimization problem for OMA transmissions in the multi-cell scenario can be written as

$$\begin{aligned}\textbf{P9:}\ \min_{P_{k,m},L^t_{k,m},t^t_{k,m}}\ & \sum_{m=1}^{M}\sum_{k=1}^{K(m)} t^t_{k,m}P_{k,m}\\ \text{s.t}\ \ & 0\le P_{k,m},\\ & \frac{\tilde{\sigma}^2_{k,m}}{\log\left(\frac{1}{1-\theta_{k,m}}\right)}\left(2^{\frac{L^t_{k,m}}{t^t_{k,m}}}-1\right)\le P^{L^t_{k,m}}_{k,m},\\ & L^{min}\le L^t_{k,m},\\ & L^t_{k,m}\le L_{k,m},\\ & \sum_{k=1}^{K(m)} L^{max}-L^t_{k,m}\le \mathcal{L}_{m,c},\\ & t^t_{k,m}\ge 0,\\ & \sum_{k=1}^{K(m)} t^t_{k,m}\le t^t.\end{aligned}$$

Clearly, **P9** is a non-convex optimization problem. In order to solve it efficiently, first we select $L^{t*}_{k,m}$ according to the solution obtained in Section IV-C. Then, **P9** can be written as

$$\begin{aligned}\textbf{P10:}\ \min_{P_{k,m},t^t_{k,m}}\ & \sum_{m=1}^{M}\sum_{k=1}^{K(m)} t^t_{k,m}P_{k,m}\\ \text{s.t}\ \ & 0\le P_{k,m},\\ & \frac{\tilde{\sigma}^2_{k,m}}{\log\left(\frac{1}{1-\theta_{k,m}}\right)}\left(2^{\frac{L^{t*}_{k,m}}{t^t_{k,m}}}-1\right)\le P^{L^{t*}_{k,m}}_{k,m},\\ & t^t_{k,m}\ge 0,\\ & \sum_{k=1}^{K(m)} t^t_{k,m}\le t^t.\end{aligned}$$

Note that the second constraint in **P10** must be active for optimality. Although **P10** is non-convex, it is a convex optimization problem with respect to $P_{k,m}$ for fixed values of $t^t_{k,m}$ and can be solved with off-the-shelf optimization tools such as CVX. However, using a special property of **P10** it can be shown that a very low complexity iterative algorithm can be used to solve it for given values of $t^t_{k,m}>0$. Toward this direction, we introduce the following notation

$$\mathbf{P}=\left[P^{L^{t*}_{1,1}}_{1,1},\ldots,P^{L^{t*}_{K,1}}_{K,1},\ldots,P^{L^{t*}_{1,M}}_{1,M},\ldots,P^{L^{t*}_{K,M}}_{K,M}\right], \quad (147)$$

$$\mathbf{t}=\left[t^t_{1,1},\ldots,t^t_{K,1},\ldots,t^t_{1,M},\ldots,t^t_{K,M}\right], \quad (148)$$

$$\Sigma_{mK+k}\left(\bar{\mathbf{P}}_{mK+k}\right)=\frac{\tilde{\sigma}^2_{k,m}}{\log\left(\frac{1}{1-\theta_{k,m}}\right)}\left(2^{\frac{L^{t*}_{k,m}}{t^t_{k,m}}}-1\right)=P^{L^{t*}_{k,m}}_{k,m}, \quad (149)$$

where $\Sigma_j(.)$ denote the j-th element of vector $\Sigma(.)$ and

$$\Sigma(\mathbf{P})=\mathbf{P},\ \ a_{k,m}=\frac{2^{\frac{L^{t*}_{k,m}}{t^t_{k,m}}}-1}{\log\left(\frac{1}{1-\theta_{k,m}}\right)}, \quad (150)$$

$$b_{k,m}=\frac{\tilde{\sigma}^2_{k,m}}{P^{L^{t*}_{k,m}}_{k,m}},\quad \eta\left(P^{L^{t*}_{k,m}}_{k,m},\bar{\mathbf{P}}_{k,m},\sigma_{k,m}\right)=a_{k,m}b_{k,m}. \quad (151)$$

With the above notations, **P10** for fixed value of $\mathbf{t}\succ\mathbf{0}$ can be written as

$$\begin{aligned}\textbf{P9:}\ \min_{\mathbf{P}}\ & \mathbf{t}^T\mathbf{P}\\ & \mathbf{P}\succeq\mathbf{0}\\ & \mathbf{P}=\Sigma(\mathbf{P}).\end{aligned}$$

Then, in the following lemma we show some important properties of $\Sigma(\mathbf{P})$.

Lemma 8: The function $\Sigma(\mathbf{P})$ has following properties

- P1: Positivity: $\Sigma(\mathbf{P})\succ 0$.
- P2: Monotonocity: If $\mathbf{P}_1\succeq\mathbf{P}_2$, then $\Sigma(\mathbf{P}_1)\succeq\Sigma(\mathbf{P}_2)$.
- P3: Scalability: If $c>1$, then $c\Sigma(\mathbf{P})\succ\Sigma(c\mathbf{P})$.

Proof: It is straight forward to prove the positivity of $\Sigma(\mathbf{P})$ using (149). Furthermore, from (149) it can be observed that any element of $\Sigma(\mathbf{P})$ increases with each element of $\mathbf{P}$. Hence, the monotonocity property is also proved. For scalability, let us assume a constant $c>1$. Moreover, without loss of generality consider the $(mK+k)$-th element of $\Sigma(\mathbf{P})$, i.e., $\Sigma_{mK+k}(\bar{\mathbf{P}}_{mK+k})$. Then, in order to prove the scalability property, we need to show that

$$c\Sigma_{mK+k}\left(\bar{\mathbf{P}}_{mK+k}\right)>\Sigma_{mK+k}\left(c\bar{\mathbf{P}}_{mK+k}\right), \quad (152)$$

is always true. Note that the inequality

$$\begin{aligned}\eta\left(P_{k,m},\bar{\mathbf{P}}_{mK+k},\sigma_{k,m}\right)&=\eta\left(cP_{k,m},c\bar{\mathbf{P}}_{mK+k},c\sigma_{k,m}\right)\\ &>\eta\left(cP_{k,m},c\bar{\mathbf{P}}_{mK+k},\sigma_{k,m}\right)\end{aligned} \quad (153)$$

always holds due to the choice of $c>1$ and the definition of $\eta(.)$ in (151). Multiplying both sides of (153) by $P_{k,m}$ we get

$$\Sigma_{mK+k}\left(\bar{\mathbf{P}}_{mK+k}\right)>\frac{\Sigma_{mK+k}\left(c\bar{\mathbf{P}}_{mK+k}\right)}{c}, \quad (154)$$

which shows that (152) is always true. This completes the proof of scalability property. ■

Based on the result of Lemma 8, it is concluded that $\Sigma(\mathbf{P})$ is the so-called standard interference function. Therefore, the iterative algorithm for power (IAP) [60] can be used to optimally solve **P11** for fixed values of $t^t_{k,m}$. The detailed steps of IAP algorithm are provided as **Algorithm 6**.

The proof of convergence for **Algorithm 6** relies on the facts that (i) $\mathbf{t}\succ\mathbf{0}$, and (ii) for any transmit power vector $\mathbf{P}'\succ\hat{\mathbf{P}}$, we have $\mathbf{t}'\prec\hat{\mathbf{t}}$, where $\mathbf{t}'$, and $\hat{\mathbf{t}}$ corresponds to transmission time vectors for $\mathbf{P}'$ and $\hat{\mathbf{P}}$, respectively.

Note that in each iteration the IAP algorithm finds the optimal value of $P^{L^{t*}_{k,m}}_{k,m}$ by using a closed-form expression. Thus, there is no search involved. This drastically reduces the complexity of the overall algorithm as compared to the CVX based approach. On the other hand, CVX uses interior point method for solving **P11** whose complexity is $\mathcal{O}((KM)^{3.5})$.

This reduction in computational complexity is crucial since the optimization over transmit powers needs to be

Algorithm 6: IAP Based Algorithm for OMA Multicell Problem for a Fixed Value of Transmit Time Allocations

Desired $t^t_{k,m}$: Choose the desired values of $t^t_{k,m}$ and save them as $t^{t\dagger}_{k,m}$;
Initialize: Chose arbitrary values of $P_{k,m}$;
Calculate: Update transmit time, $t^t_{k,m}$, of each user for the arbitrary $P^{L^{t*}_{k,m}}_{k,m}$;
Calculate: $\hat{\sigma}_{k,m}$ for all the users;
for $I = 1{:}I_{max}$ **do**
  if $\|\mathbf{t} - \mathbf{t}^{\dagger}\|^2 \geq \epsilon$ **then**
    Obtain $P^{L^t_{k,m}}_{k,m}$ of all the users with transmit times $t^{t\dagger}_{k,m}$;
    Update $\tilde{\sigma}_{k,m}$ for all the users;
    Update $t^t_{k,m}$ according to updated $P^{L^t_{k,m}}_{k,m}$ and $\tilde{\sigma}_{k,m}$;
  end
  else
    Output $P^{L^t_{k,m}}_{k,m}$ as the optimal power allocations for $t^{t\dagger}_{k,m}$
  end
end

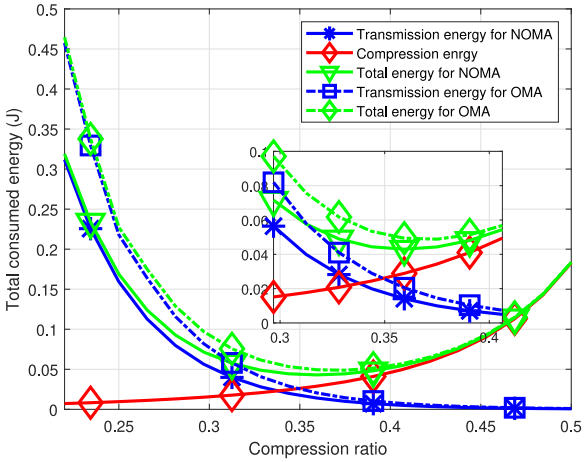

FIGURE 3. Total energy consumption with respect to different compression ratios for zero SIC imperfections.

TABLE 3. Simulation parameters for single-cell with perfect SIC.

Parameter	value	Parameter	value
K	4	n	2
Bandwidth	20 MHz	L_{max}	8
$\{d_1, d_2, d_3, d_4\}$	$\{10, 15, 20, 25\}$ m	L_{min}	4
$\{\theta_1, \theta_2, \theta_3, \theta_4\}$	$\{.1, .15, .2, .25\}$	σ_k^2	-110 dBm
ϵ	4	ϱ	10^{-13} J

performed over all possible values of the compression ratio which can result in much higher overall computational complexity if the underlying transmit power optimization algorithm has high computational complexity.

VI. SIMULATION RESULTS

This section provides the simulation results to assess the performance improvements obtained due to the application of proposed energy minimization algorithms presented in the previous sections. This section is divided into three subsections. Section VI-A discusses the single-cell scenario with perfect SIC. The simulation results corresponding to imperfect SIC for single-cell scenario are provided in Section VI-B. Finally, Section VI-C provides the simulation results corresponding to multi-cell scenario. The resulting optimization problems in each scenario have different feasible regions, and therefore for each scenario we have chosen different simulation parameters to illustrate the effectiveness of the proposed algorithms. Hence, the values of the simulations parameters for each scenario are given in tabular form in its respective subsection.

A. SINGLE-CELL WITH PERFECT SIC SCENARIO

For this subsection, unless otherwise specified, the values of important simulation parameters are provided in Table 3. Fig. 3 shows the total energy consumption for various compression ratios with NOMA and OMA transmissions. For both transmission schemes, it can be easily observed that significant savings in terms of total energy consumption can be realized by choosing an appropriate value of compression ratio. This is due to the fact that for smaller values of compression ratio, the transmission energy is higher and it dominates the total energy consumption. On the other hand, for larger values of compression ratio, the compression energy is higher and it causes the total energy consumption to increase. Overall, there exists an optimal value of compression ratio which can minimize the sum total of compression and transmission energy. This optimal value of the compression ratio can be obtained by performing a linear search over all the possible values of compression ratio as suggested by **Algorithm 2** and **Algorithm 3** for NOMA and OMA transmissions, respectively.

The savings in total energy consumption for different values L_{max} and $L_{min} = 0.5L_{max}$ are illustrated in Fig. 4. As we can see, the percentage savings are small for smaller L_{max} while they become significantly large for higher values of L_{max}. This is because smaller values of L_{max} cause smaller transmission energy consumption and hence smaller margin for improvements are brought by the compression. This ultimately leads to a smaller gain in overall energy savings. On the other hand, for larger values of L_{max} more margin for savings in transmission energy is available and hence we observe a higher gain in savings of total energy consumption.

Next, in Fig. 5 we demonstrate the savings in total energy consumption for different outage probability requirements. For this result, we assume θ_k are same for all the DUs. This means, for example, the second (from left) red circle is obtained by setting $\theta_1 = \theta_2 = \theta_3 = \theta_4 = 0.15$ in the optimization problems **P1** and **P2**. We can see that savings

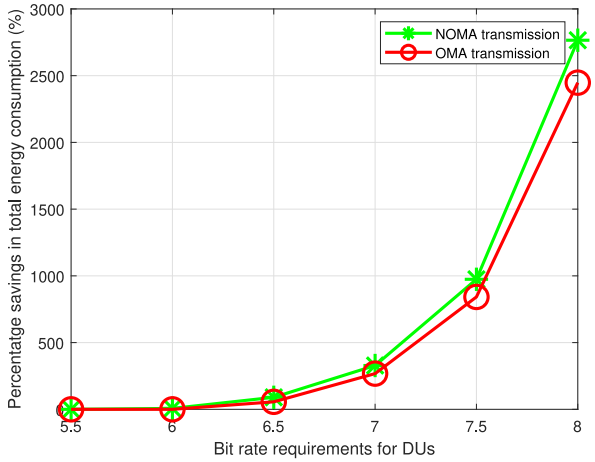

FIGURE 4. Energy savings with respect to different bit rate requirements.

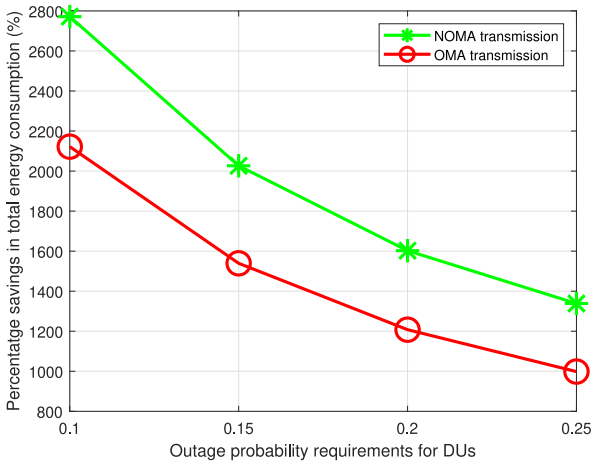

FIGURE 5. Energy savings with respect to different outage probability requirements.

are much larger for stricter outage constraints while comparatively smaller for more relaxed outage constraints. This behavior can be explained as follows. In order to meet stricter outage constraints, more transmission energy is required and hence a reduction in transmission energy brought by performing the compression can significantly reduce the transmission energy by reducing the transmission rate. This leads to a higher savings in total energy consumption. On the contrary, for more relaxed outage constraints the transmission energy is comparatively smaller and hence comparatively smaller improvement can be realized through compression.

B. SINGLE-CELL SCENARIO WITH IMPERFECT SIC

For this subsection, unless otherwise specified, the values of important simulation parameters for single-cell scenario with imperfect SIC are provided in Table 4. Fig. 6 shows the total energy consumption results for different compression ratio when $\varkappa = 0.05$. Again, it can be easily observed that there exists an optimal value of the compression ratio which minimizes the total energy consumption. The underlying reasons for existence of such an optimal value

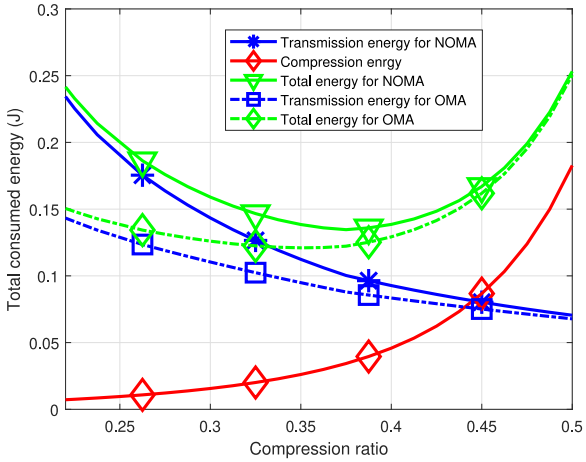

FIGURE 6. Total energy consumption with respect to different compression ratios for non-zero SIC imperfections.

TABLE 4. Simulation parameters for single-cell with imperfect SIC.

Parameter	value	Parameter	value
$\varkappa$	$\{.01, .05, .1, .15\}$	n	3
Bandwidth	160 MHz	L_{max}	1
$\{d_1, d_2, d_3, d_4\}$	$\{220, 320, 430, 530\}$ m	L_{min}	.5
$\{\theta_1, \theta_2, \theta_3, \theta_4\}$	$\{.1, .15, .2, .25\}$	σ_k^2	-110 dBm
ϵ	4	ϱ	10^{-13} J

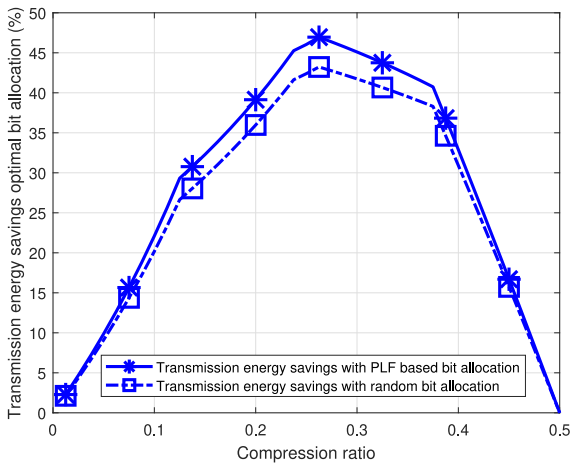

FIGURE 7. Total energy consumption savings with respect to different compression ratios for non-zero SIC imperfections.

of compression ratio are similar to those discussed in Section VI-A and are hence omitted here for brevity.

Since we have proposed to use same transmission bit allocation for imperfect SIC scenario as used for perfect SIC scenario, we illustrate the advantage of using a suboptimal transmission bit allocation to the proposed transmission bit allocations in Fig. 7. It can be observed that the use of proposed transmission bit allocation among DUs results in significant gains in total energy savings. While it is not possible to prove the optimality of the proposed transmission bit allocations, the result shown in Fig. 7 verifies that the

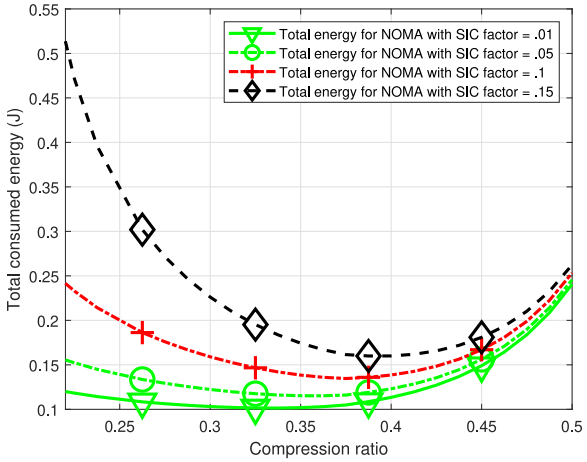

FIGURE 8. Total energy consumption with respect to different compression ratios for various SIC factors.

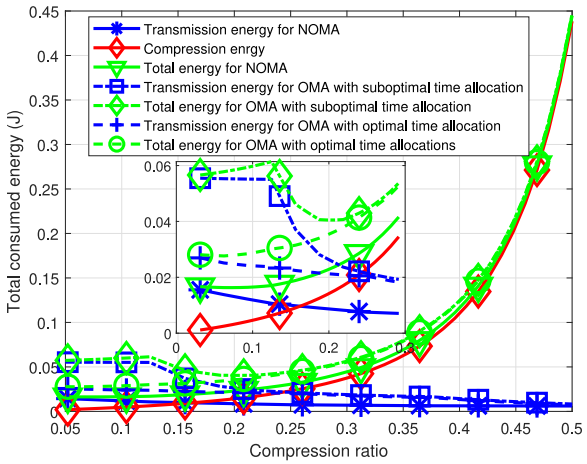

FIGURE 9. Total energy consumption with respect to different compression ratios for multi-cell scenario.

proposed transmission bit allocation significantly enhances the total energy savings.

The affect of different SIC factors, $\varkappa$, on the total energy consumption is illustrated in Fig. 8. Note that a higher value of $\varkappa$ corresponds to more severe imperfection in SIC. It can be easily inferred that the savings in total energy are higher for a higher value of $\varkappa$. This is due to the fact that a higher degradation in SIC will result in higher interference power which will cause the transmission power to increase in order to meet the QoS constraints. This effect is more pronounced when a higher transmission data rate is required due to the higher transmission power. However, thanks to the compression the transmission data rate can be lowered which lowers the transmission energy thus resulting in a reduction of the total energy consumption.

C. MULTI-CELL SCENARIO

The simulation parameters used to obtain the results for multi-cell scenario are provided in Table 5. Fig. 9 shows the total energy consumption as a function of compression

TABLE 5. Simulation parameters for multi-cell scenario.

Parameter	value	Parameter	value
M	3	n	5
$\{K(1), K(2), K(3)\}$	$\{4, 4, 4\}$	L_{max}	.8
$\{d_1, d_2, d_3, d_4\}$	$\{10, 15, 20, 25\}$ m	L_{min}	.4
$\{\theta_1, \theta_2, \theta_3, \theta_4\}$	$\{.1, .15, .2, .25\}$	σ_k^2	-110 dBm
$\{\hat{d}_1^2, \hat{d}_1^3\}$	$\{500, 500\}$ m	Bandwidth	160 MHz
$\{\hat{d}_2^2, \hat{d}_2^3\}$	$\{450, 450\}$ m	ϵ	4
$\{\hat{d}_3^2, \hat{d}_3^3\}$	$\{400, 400\}$ m	$\{\hat{d}_4^2, \hat{d}_4^3\}$	$\{350, 350\}$ m

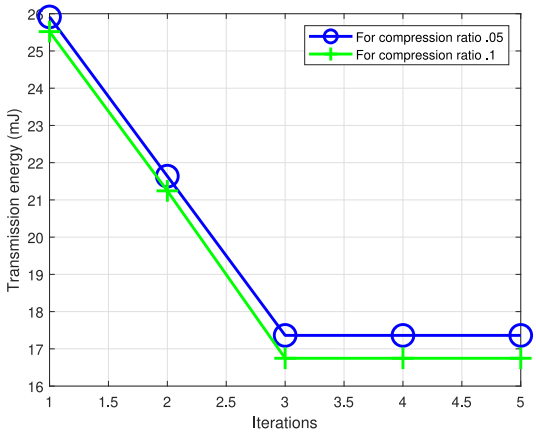

FIGURE 10. Convergence result for Algorithm 5.

ratio. It can be seen that there exists an optimal compression ratio which minimizes the total energy consumption for both NOMA and OMA transmissions. Moreover, it can also be observed that the choice of transmit time allocations greatly affects the overall energy consumption. In fact, it can be easily observed from Fig. 9 that choosing the time allocation as suggested in Section IV-C results in a savings of about 31% in total energy consumption on top of the savings achieved due to compression.

Finally, since **Algorithm 5** and **Algorithm 6** are iterative algorithms, the convergence and monotonocity of the achieved objective values is an important performance metric. Therefore, Fig. 10 and Fig. 11 depict the convergence results for **Algorithm 5** and **Algorithm 6**, respectively. We can see that the objective values achieved in successive iterations are non-increasing for both algorithms. In addition, both algorithms converge within only a few iterations. Specifically, **Algorithm 5** converges after 3 iterations. This is due to the fact that in each iteration **Algorithm 5** uses **Algorithm 1** to minimize the transmission energy of the individual BSs and since we assumed 3 BSs in our simulation setup the algorithm successively achieves a lower objective value in each of the first three iterations. After the first three iterations no more reduction in the objective value can be achieved and hence convergence is attained after three iterations. On the other hand, **Algorithm 6** minimizes the transmission energy for all the BSs in each iteration. Therefore, we observe that **Algorithm 6** converges after only two iteration.

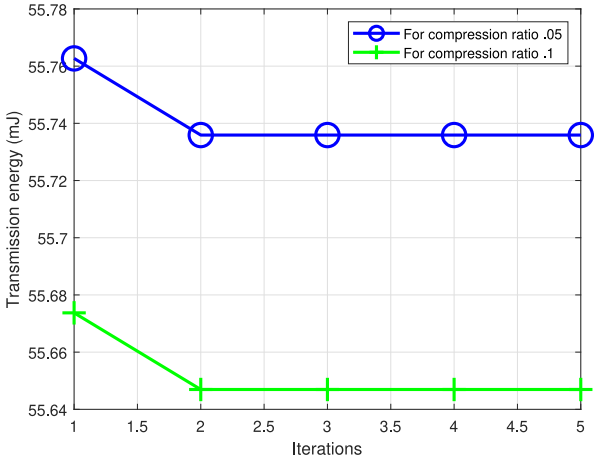

FIGURE 11. Convergence result for Algorithm 6.

VII. CONCLUSION

This paper studied the combination of compression with communication to achieve total energy minimization at the BSs while guaranteeing the QoS constraints of individual DUs. The goal of minimizing the total energy minimization is achieved for both NOMA and OMA transmission schemes in single and multi-cell scenarios. The formulated problems are non-convex and difficult to solve, however for both transmission schemes, it is revealed with the help of convex optimization techniques that the optimal solutions depend on the PLFs of individual DUs. Specifically, if the PLFs are arranged in a descending order then there exists a user with index $\hat{k}$ such that full compression is applied for all the users with index in the set $\{1, \ldots, \hat{k}-1\}$ and no compression is applied for all the users in the set $\{\hat{k}+1, \ldots, K\}$. Based on this observation, low-complexity optimization algorithms are developed for single cell scenario. The observation about PLFs is then used to obtain low complexity iterative algorithms for multi-cell scenario. The convergence of these iterative algorithms are also proved theoretically and with simulations. Simulations results also demonstrated that considerable savings in the total energy consumption can be achieved if compression is done at the BSs before transmission.

REFERENCES

[1] M. Elbayoumi, M. Kamel, W. Hamouda, and A. Youssef, "NOMA-assisted machine-type communications in UDN: State-of-the-art and challenges," *IEEE Commun. Surveys Tuts.*, vol. 22, no. 2, pp. 1276–1304, 2nd Quart., 2020.

[2] D. Moltchanov, E. Sopin, V. Begishev, A. Samuylov, Y. Koucheryavy, and K. Samouylov, "A tutorial on mathematical modeling of 5G/6G millimeter wave and Terahertz cellular systems," *IEEE Commun. Surveys Tuts.*, vol. 24, no. 2, pp. 1072–1116, 2nd Quart., 2022.

[3] H. A. Ammar, R. Adve, S. Shahbazpanahi, G. Boudreau, and K. V. Srinivas, "User-centric cell-free massive MIMO networks: A survey of opportunities, challenges and solutions," *IEEE Commun. Surveys Tuts.*, vol. 24, no. 1, pp. 611–652, 1st Quart., 2022.

[4] M. Vaezi et al., "Cellular, wide-area, and non-terrestrial IoT: A survey on 5G advances and the road toward 6G," *IEEE Commun. Surveys Tuts.*, vol. 24, no. 2, pp. 1117–1174, 2nd Quart., 2022.

[5] Y. Liu, X. Liu, X. Mu, T. Hou, J. Xu, M. Di Renzo, and N. Al-Dhahir, "Reconfigurable intelligent surfaces: Principles and opportunities," *IEEE Commun. Surveys Tuts.*, vol. 23, no. 3, pp. 1546–1577, 3rd Quart., 2021.

[6] A. Memedi and F. Dressler, "Vehicular visible light communications: A survey," *IEEE Commun. Surveys Tuts.*, vol. 23, no. 1, pp. 161–181, 1st Quart., 2021.

[7] Z. Ding, P. Fan, and H. V. Poor, "Impact of user pairing on 5G nonorthogonal multiple-access downlink transmissions," *IEEE Trans. Veh. Tech.*, vol. 65, no. 8, pp. 6010–6023, Aug. 2016.

[8] F. Fang, Y. Xu, Z. Ding, C. Shen, M. Peng, and G. K. Karagiannidis, "Optimal resource allocation for delay minimization in NOMA-MEC networks," *IEEE Trans. Commun.*, vol. 68, no. 12, pp. 7867–7881, Dec. 2020.

[9] L. Xu, W. Yin, X. Zhang, and Y. Yang, "Fairness-aware throughput maximization over cognitive heterogeneous NOMA networks for industrial cognitive IoT," *IEEE Trans. Commun.*, vol. 68, no. 8, pp. 4723–4733, Aug. 2020.

[10] I.-H. Lee and H. Jung, "User selection and power allocation for downlink NOMA systems with quality-based feedback in Rayleigh fading channels," *IEEE Wireless Commun. Lett.*, vol. 9, no. 11, pp. 1924–1927, Nov. 2020.

[11] Z. Yang, W. Xu, C. Pan, Y. Pan, and M. Chen, "On the optimality of power allocation for NOMA downlinks with individual QoS constraints," *IEEE Commun. Lett.*, vol. 21, no. 7, pp. 1649–1652, Jul. 2017.

[12] F. Liu and M. Petrova, "Dynamic power allocation for downlink multi-carrier NOMA systems," *IEEE Commun. Lett.*, vol. 22, no. 9, pp. 1930–1933, Sep. 2018.

[13] M. Ashraf and L. Vandendorpe, "Rate maximizing online power allocation at energy harvesting transmitter for multiple receivers," in *Proc. IEEE Int. Conf. Commun. (ICC)*, 2020, pp. 1–7.

[14] M. Ashraf, Z. Wang, and L. Vandendorpe, "Online power allocation at energy harvesting transmitter for multiple receivers with and without individual rate constraints for OMA and NOMA transmissions," *IEEE Trans. Green Commun. Net.*, vol. 5, no. 3, pp. 1594–1609, Sep. 2021.

[15] Y. Fu, L. Salaün, C. W. Sung, and C. S. Chen, "Subcarrier and power allocation for the downlink of multicarrier NOMA systems," *IEEE Trans. Veh. Tech.*, vol. 67, no. 12, pp. 11833–11847, Dec. 2018.

[16] S. Mounchili and S. Hamouda, "Pairing distance resolution and power control for massive connectivity improvement in NOMA systems," *IEEE Trans. Veh. Tech.*, vol. 69, no. 4, pp. 4093–4103, Apr. 2020.

[17] I. Randrianantenaina, M. Kaneko, H. Dahrouj, H. ElSawy, and M.-S. Alouini, "Interference management in NOMA-based fog-radio access networks via scheduling and power allocation," *IEEE Trans. Commun.*, vol. 68, no. 8, pp. 5056–5071, Aug. 2020.

[18] L. Zhu, J. Zhang, Z. Xiao, X. Cao, D. O. Wu, and X.-G. Xia, "Millimeter-wave NOMA with user grouping, power allocation and hybrid beamforming," *IEEE Trans. Wireless Comm.*, vol. 18, no. 11, pp. 5065–5079, Nov. 2019.

[19] J. Zuo, Y. Liu, Z. Qin, and N. Al-Dhahir, "Resource allocation in intelligent reflecting surface assisted NOMA systems," *IEEE Trans. Commun.*, vol. 68, no. 11, pp. 7170–7183, Nov. 2020.

[20] G. Wang, Y. Shao, L.-K. Chen, and J. Zhao, "Subcarrier and power allocation in OFDM-NOMA VLC systems," *IEEE Photon. Tech. Lett.*, vol. 33, no. 4, pp. 189–192, Feb. 2021.

[21] K. Yang, X. Yan, Q. Wang, H.-C. Wu, and K. Qin, "Joint power allocation and relay beamforming optimization for weighted sum-rate maximization in NOMA AF relay system," *IEEE Commun. Lett.*, vol. 25, no. 1, pp. 219–223, Jan. 2021.

[22] W. U. Khan et al., "Integration of NOMA with reflecting intelligent surfaces: A multi-cell optimization with SIC decoding errors," *IEEE Trans. Green Commun. Netw.*, vol. 7, no. 3, pp. 1554–1565, Sep. 2023.

[23] W. U. Khan, F. H. Memon, K. Dev, M. A. Javed, D.-T. Do, and N. M. F. Qureshi, "Ambient BackCom in beyond 5G NOMA networks: A multi-cell resource allocation framework," *Digt. Commun. Net.*, vol. 8, no. 6, pp. 1005–1013, 2022. [Online]. Available: https://www.sciencedirect.com/science/article/pii/S2352864822002371

[24] W. U. Khan, F. Jameel, X. Li, M. Bilal, and T. A. Tsiftsis, "Joint spectrum and energy optimization of NOMA-enabled small-cell networks with QoS guarantee," *IEEE Trans. Veh. Tech.*, vol. 70, no. 8, pp. 8337–8342, Aug. 2021.

[25] X. Li, C. Li, and Y. Jin, "Dynamic resource allocation for transmit power minimization in OFDM-based NOMA systems," *IEEE Commun. Lett.*, vol. 20, no. 12, pp. 2558–2561, Dec. 2016.
[26] D. Ni, L. Hao, Q. T. Tran, and X. Qian, "Transmit power minimization for downlink multi-cell multi-carrier NOMA networks," *IEEE Commun. Lett.*, vol. 22, no. 12, pp. 2459–2462, Dec. 2018.
[27] J. Zhu, Y. Huang, J. Wang, K. Navaie, and Z. Ding, "Power efficient IRS-assisted NOMA," *IEEE Trans. Commun.*, vol. 69, no. 2, pp. 900–913, Feb. 2021.
[28] Z. Wei, D. W. K. Ng, J. Yuan, and H.-M. Wang, "Optimal resource allocation for power-efficient MC-NOMA with imperfect channel state information," *IEEE Trans. Commun.*, vol. 65, no. 9, pp. 3944–3961, Sep. 2017.
[29] W. U. Khan, M. A. Jamshed, E. Lagunas, S. Chatzinotas, X. Li, and B. Ottersten, "Energy efficiency optimization for backscatter enhanced NOMA cooperative V2X communications under imperfect CSI," *IEEE Trans. Intell. Trans. Syst.*, vol. 24, no. 11, pp. 12961–12972, Nov. 2023.
[30] W. U. Khan, X. Li, A. Ihsan, Z. Ali, B. M. Alhalawany, and G. A. S. Sidhu, "Energy efficiency maximization for beyond 5G NOMA-enabled heterogeneous networks," *Peer-to-Peer Netw. Appl.*, vol. 14, pp. 3250–3264, 2021, doi: 10.1007/s12083-021-01176-5.
[31] M. R. Zamani, M. Eslami, M. Khorramizadeh, and Z. Ding, "Energy-efficient power allocation for NOMA with imperfect CSI," *IEEE Trans. Veh. Tech.*, vol. 68, no. 1, pp. 1009–1013, Jan. 2019.
[32] C. Chen, S. Fu, X. Jian, M. Liu, X. Deng, and Z. Ding, "NOMA for energy-efficient LiFi-enabled bidirectional IoT communication," *IEEE Trans. Commun.*, vol. 69, no. 3, pp. 1693–1706, Mar. 2021.
[33] W. U. Khan, A. Ihsan, T. N. Nguyen, Z. Ali, and M. A. Javed, "NOMA-enabled backscatter communications for green transportation in automotive-industry 5.0," *IEEE Trans. Ind. Informat.*, vol. 18, no. 11, pp. 7862–7874, Nov. 2022.
[34] A. Ihsan, W. Chen, W. U. Khan, Q. Wu, and K. Wang, "Energy-efficient backscatter aided uplink NOMA roadside sensor communications under channel estimation errors," *IEEE Trans. Intell. Trans. Sys.*, vol. 24, no. 5, pp. 4962–4974, May 2023.
[35] I. Cosandal, M. Koca, E. Biglieri, and H. Sari, "NOMA-2000 versus PD-NOMA: An outage probability comparison," *IEEE Commun. Lett.*, vol. 25, no. 2, pp. 427–431, Feb. 2021.
[36] B. Xu, Z. Xiang, P. Ren, and X. Guo, "Outage performance of downlink full-duplex network-coded cooperative NOMA," *IEEE Wireless Commun. Lett.*, vol. 10, no. 1, pp. 26–29, Jan. 2021.
[37] M. Hedayati and I.-M. Kim, "CoMP-NOMA in the SWIPT networks," *IEEE Trans. Wireless Commun.*, vol. 19, no. 7, pp. 4549–4562, Jul. 2020.
[38] M. Salehi, H. Tabassum, and E. Hossain, "Meta distribution of SIR in large-scale uplink and downlink NOMA networks," *IEEE Trans. Comm.*, vol. 67, no. 4, pp. 3009–3025, Apr. 2019.
[39] J. Zheng, Q. Zhang, and J. Qin, "Average block error rate of downlink NOMA short-packet communication systems in Nakagami-*m* fading channels," *IEEE Commun. Lett.*, vol. 23, no. 10, pp. 1712–1716, Oct. 2019.
[40] F. Fang, J. Cheng, and Z. Ding, "Joint energy efficient subchannel and power optimization for a downlink NOMA heterogeneous network," *IEEE Trans. Veh. Tech.*, vol. 68, no. 2, pp. 1351–1364, Feb. 2019.
[41] S. Timotheou and I. Krikidis, "Fairness for non-orthogonal multiple access in 5G systems," *IEEE Sign. Proc. Lett.*, vol. 22, no. 10, pp. 1647–1651, Oct. 2015.
[42] S. Shi, L. Yang, and H. Zhu, "Outage balancing in downlink nonorthogonal multiple access with statistical channel state information," *IEEE Trans. Wireless Commun.*, vol. 15, no. 7, pp. 4718–4731, Jul. 2016.
[43] F. Kara and H. Kaya, "Threshold-based selective cooperative NOMA: Capacity/outage analysis and a joint power allocation-threshold selection optimization," *IEEE Commun. Lett.*, vol. 24, no. 9, pp. 1929–1933, Sep. 2020.
[44] V. Mandawaria, E. Sharma, and R. Budhiraja, "Energy-efficient massive MIMO multi-relay NOMA systems with CSI errors," *IEEE Trans. Commun.*, vol. 68, no. 12, pp. 7410–7428, Dec. 2020.
[45] J. Cui, Z. Ding, and P. Fan, "Outage probability constrained MIMO-NOMA designs under imperfect CSI," *IEEE Trans. Wireless Commun.*, vol. 17, no. 12, pp. 8239–8255, Dec. 2018.
[46] A. Chatzipapas, S. Alouf, and V. Mancuso, "On the minimization of power consumption in base stations using on/off power amplifiers," in *Proc. IEEE Online Conf. Green Commun.*, 2011, pp. 18–23.
[47] M. Nasir, G. Christine, and A. Rashid, "5.6-the JPEG lossless image compression standards," in *Handbook of Image and Video Processing* (Communications, Networking and Multimedia), 2nd ed., A. Bovik, Eds. Burlington, MA, USA: Academic, 2005, pp. 733–745. [Online]. Available: https://www.sciencedirect.com/science/article/pii/B9780121197926501066
[48] J.-B. Wang, J. Zhang, C. Ding, H. Zhang, M. Lin, and J. Wang, "Joint optimization of transmission bandwidth allocation and data compression for mobile-edge computing systems," *IEEE Commun. Lett.*, vol. 24, no. 10, pp. 2245–2249, Oct. 2020.
[49] X. Li, C. You, S. Andreev, Y. Gong, and K. Huang, "Wirelessly powered crowd sensing: Joint power transfer, sensing, compression, and transmission," *IEEE J. Sel. Areas Commun.*, vol. 37, no. 2, pp. 391–406, Feb. 2019.
[50] I. Rais, D. Balouek-Thomert, A.-C. Orgerie, L. Lefevre, and M. Parashar, "Leveraging energy-efficient non-lossy compression for data-intensive applications," in *Proc. Int. Conf. High Perform. Comput. Simul. (HPCS)*, 2019, pp. 463–469.
[51] K. C. Barr and K. Asanović, "Energy-aware lossless data compression," *ACM Trans. Comput. Syst.*, vol. 24, no. 3, pp. 250–291, Aug. 2006, doi: 10.1145/1151690.1151692.
[52] A. Milenkovic, A. Dzhagaryan, and M. Burtscher, "Performance and energy consumption of lossless compression/decompression utilities on mobile computing platforms," in *Proc. IEEE 21st Int. Symp. Model., Anal. Simul. Comput. Telecommun. Syst.*, 2013, pp. 254–263.
[53] S. Cui, A. Goldsmith, and A. Bahai, "Energy-efficiency of MIMO and cooperative MIMO techniques in sensor networks," *IEEE J. Sel. Areas Commun.*, vol. 22, no. 6, pp. 1089–1098, Aug. 2004.
[54] M. Ashraf, J. Jung, H. M. Shin, and I. Lee, "Energy efficient online power allocation for two users with energy harvesting," *IEEE Signal Processing Lett.*, vol. 26, no. 1, pp. 24–28, Jan. 2019.
[55] S. Boyd and L. Vandenberghe, *Convex Optimization*. Cambridge, U.K.: Cambridge Univ. Press, 2004.
[56] S. Yu, W. U. Khan, X. Zhang, and J. Liu, "Optimal power allocation for NOMA-enabled D2D communication with imperfect SIC decoding," *Phys. Commun.*, vol. 46, Jun. 2021, Art. no. 101296. [Online]. Available: https://www.sciencedirect.com/science/article/pii/S1874490721000331
[57] M. Asif, A. Ihsan, W. U. Khan, A. Ranjha, S. Zhang, and S. X. Wu, "Energy-efficient backscatter-assisted coded cooperative NOMA for B5G wireless communications," *IEEE Trans. Green Commun. Netw.*, vol. 7, no. 1, pp. 70–83, Mar. 2023.
[58] X. Li et al., "Hardware impaired ambient backscatter NOMA systems: Reliability and security," *IEEE Trans. Commun.*, vol. 69, no. 4, pp. 2723–2736, Apr. 2021.
[59] D. Veberic, "Having fun with Lambert W(x) function," 2018, *arXiv:1003.1628v2*.
[60] C. K. Ho, D. Yuan, L. Lei, and S. Sun, "Power and load coupling in cellular networks for energy optimization," *IEEE Trans. Wireless Commun.*, vol. 14, no. 1, pp. 509–519, Jan. 2015.